AWARD NUMBER: W81XWH-12-1-0153

TITLE: "Probing Androgen Receptor Signaling in Circulating Tumor Cells in Prostate Cancer"

PRINCIPAL INVESTIGATOR: David T. Miyamoto, MD, PhD

CONTRACTING ORGANIZATION: Massachusetts General Hospital
Boston, MA 02114-2621

REPORT DATE: July 2016

TYPE OF REPORT: Annual Summary

PREPARED FOR: U.S. Army Medical Research and Materiel Command
Fort Detrick, Maryland 21702-5012

REPORT DOCUMENTATION PAGE

Form Approved
OMB No. 0704-0188

1. REPORT DATE	2. REPORT TYPE	3. DATES COVERED
July 2016	Annual Summary	1 July 2015 - 30 June 2016

4. TITLE AND SUBTITLE
Probing Androgen Receptor Signaling in Circulating Tumor Cells in Prostate Cancer

5a. CONTRACT NUMBER

5b. GRANT NUMBER
W81XWH-12-1-0153

5c. PROGRAM ELEMENT NUMBER

6. AUTHOR(S)
David T. Miyamoto

E-Mail: dmiyamoto@partners.org

5d. PROJECT NUMBER

5e. TASK NUMBER

5f. WORK UNIT NUMBER

7. PERFORMING ORGANIZATION NAME(S) AND ADDRESS(ES)

Massachusetts General Hospital
55 Fruit Street
Boston, MA 02114-2621

8. PERFORMING ORGANIZATION REPORT NUMBER

9. SPONSORING / MONITORING AGENCY NAME(S) AND ADDRESS(ES)
U.S. Army Medical Research and Materiel Command
Fort Detrick, Maryland 21702-5012

10. SPONSOR/MONITOR'S ACRONYM(S)

11. SPONSOR/MONITOR'S REPORT NUMBER(S)

12. DISTRIBUTION / AVAILABILITY STATEMENT

Approved for Public Release; Distribution is Unlimited

13. SUPPLEMENTARY NOTES

14. ABSTRACT

This Physician Research Training Award supports a mentored training program integrated with a research project focused on the study of circulating tumor cells (CTCs) in prostate cancer patients using a microfluidic device ("CTC-chip") to isolate CTCs from peripheral blood samples. During this award, we have developed a quantitative immunofluorescence assay to measure AR activity in single CTCs in patients with metastatic prostate cancer receiving treatment with hormonal therapy. We have also developed methods for single CTC RNA-seq and digital gene expression profiling, and have applied these techniques to single CTCs. We have analyzed single cell transcriptomes to reveal the heterogeneity of CTCs, and to identify key genes and molecular pathways enriched in CTCs that may contribute to treatment resistance in prostate cancer, including the non-canonical Wnt pathway. Finally, this Award has enabled the protection of time for research and mentored training of the PI to continue his development towards a productive independent career in translational prostate cancer research.

15. SUBJECT TERMS
prostate cancer, circulating tumor cells, androgen receptor, castration-resistant prostate cancer, RNA sequencing, single cell

16. SECURITY CLASSIFICATION OF:			17. LIMITATION OF ABSTRACT	18. NUMBER OF PAGES	19a. NAME OF RESPONSIBLE PERSON
a. REPORT	b. ABSTRACT	c. THIS PAGE			USAMRMC
Unclassified	Unclassified	Unclassified	Unclassified	46	19b. TELEPHONE NUMBER *(include area code)*

Table of Contents

Page

1. Introduction…….4

2. Keywords…….4

3. Overall Project Summary……..5

4. Key Research Accomplishments……10

5. Conclusion……10

6. Publications, Abstracts, and Presentations…….…….11

7. Inventions, Patents and Licenses……11

8. Reportable Outcomes..……12

9. Other Achievements……12

10. References……13

11. Appendices……..14

INTRODUCTION

Castration-resistant prostate cancer (CRPC) is thought to arise from the persistence of androgen receptor (AR) signaling in cancer cells despite castrate levels of testosterone (1). As second line AR targeting therapies have entered clinical care for CRPC (e.g. abiraterone acetate and enzalutamide) in addition to cytotoxic therapeutics (e.g. docetaxel, cabazitaxel, Ra-223), no reliable biomarkers exist to target appropriate therapies to individual patients (2, 3). In the Research Project supported by this Physician Research Training Award, we use a novel microfluidic technology (the "CTC-chip") to interrogate the status of AR signaling and other signaling pathways in circulating tumor cells (CTCs) isolated from metastatic prostate cancer patients in an effort to develop novel biomarkers to guide therapy, as well as to understand the biology of CRPC. An AR activity signature developed in prostate cancer cell lines is being applied to CTCs in patients with castration-resistant prostate cancer (CRPC) before and after secondary hormonal therapies to test the hypothesis that effective suppression of AR signaling in CTCs correlates with clinical response to hormonal therapy. To identify novel genes and pathways involved in the evolution of treatment resistant disease, digital gene expression profiling of single CTCs is being performed. These studies are aimed at providing initial validation of novel molecular biomarkers that can monitor and predict responses to second-line hormonal therapy in patients with CRPC, as well as revealing insights into the mechanisms underlying treatment resistance in prostate cancer. In combination with this integrated research project, this Physician Research Training Award enables the PI to have protected time for research and mentored training towards his development into an independent translational prostate cancer researcher.

Specific Aims

1. Define an AR activity score in CTCs and test the hypothesis that AR signaling activity in prostate CTCs correlates with response to second-line hormonal therapy in metastatic prostate cancer patients.

2. Perform digital gene expression (DGE) profiling of prostate CTCs to identify novel pathways that promote castration resistance.

KEY WORDS

prostate cancer, circulating tumor cells, androgen receptor, castration-resistant prostate cancer, RNA sequencing, single cell

OVERALL PROJECT SUMMARY

Progress on Statement of Work (SOW).

As described in previous Annual Progress Reports for this Research Project, we have developed a single cell immunofluorescence-based assay for measurement of AR activity in CTCs, and have demonstrated feasibility of using this assay as a potential biomarker to monitor and predict response to second line hormonal therapy in patients with castration-resistant prostate cancer (CRPC) (4, 5). We have also demonstrated feasibility of performing high throughput qRT-PCR and whole transcriptome RNA-sequencing of single prostate CTCs, using a 3rd generation CTC isolation platform, the CTC-iChip (6, 7). Progress during the current reporting period of this Project has focused on the demonstration of our ability to obtain high quality whole transcriptome RNA-seq data from single CTCs. We have now applied this single cell RNA-seq technique to CTCs isolated from patients with prostate cancer. We have engaged in extensive bioinformatic analyses to identify molecular pathways that are enriched in CTCs, resulting in identification of the non-canonical Wnt signaling pathway as significantly associated with treatment resistance. These studies have resulting in a manuscript that was published in *Science* during this reporting period (8) (see Appendix). Ongoing studies are aimed at further validation of the CTC AR activity assay, further exploration of the non-canonical Wnt signaling pathway as a mechanism of anti-androgen resistance, and continued analysis of transcriptional profiles of CTCs to provide insights into the molecular mechanisms of treatment resistance in CRPC.

Progress on Tasks related to the Research Project are outlined below.

Task 1. Regulatory review and approval of clinical protocol.

A clinical research protocol for the collection of blood from patients with solid tumors for CTC analysis (DF/HCC 05-300) was initially received by the US Army Medical Research and Materiel Command (USAMRMC), Office of Research Protections (ORP), Human Research Protection Office (HRPO) on 9 May 2012, and reviewed for compliance with human subject protection requirements. A revised research consent form and clinical research protocol was approved by the HRPO on 7 June 2012, and this revised protocol was approved by the Dana-Farber Cancer Institute Institutional Review Board (DFCI IRB) on 12 July 2012. The final protocol received approval by the HRPO on 30 July 2012. Continuation of the subject protocol was approved by the DFCI IRB on 30 May 2013, 9 May 2014, 17 June 2015, and most recently on 30 May 2016. This approval is due for continuing review by the DFCI IRB on 28 March 2017.

Task 2. (Aim 1) Recruitment of patients with castration-resistant prostate cancer for CTC AR activity analysis.

During this reporting period, additional patients with CRPC were recruited for the purposes of AR activity analysis in CTCs. Of note, the overall accrual rate was slower than initially anticipated due to a transition in CTC isolation technology in the laboratory from the 2nd generation HB CTC-chip technology (9) to the 3rd generation CTC iChip technology (6). However, now that this technology has been incorporated into the laboratory, it is anticipated that the goal subject accrual will be met during the remainder of this project.

Task 3. (Aim 1) CTC AR signature activity analysis in patients.

As part of this Research Project, we developed a novel CTC-based single cell immunophenotyping approach to measure AR activity in CTCs using two genes that we identified as most consistently upregulated and downregulated following AR modulation in prostate cancer cells: PSA (androgen driven) and PSMA (androgen suppressed). Since the publication of our initial validation of this assay (4), which was based on CTC isolation using the 2nd generation HB CTC-chip technology (9), we transitioned the laboratory to the 3rd generation CTC iChip technology (6), and have adapted the PSA/PSMA assay for use with this new CTC isolation platform. During this reporting period, we have continuing our efforts to apply this assay in castration-resistant prostate cancer patients receiving second-line hormonal therapy (see Task 2). Data analysis for this cohort of patients is ongoing.

Task 4. (Aim 2) Recruitment of patients with metastatic castration-resistant prostate cancer and metastatic castration-sensitive prostate cancer for digital gene expression profiling.

We have recruited 24 patients with metastatic prostate cancer and 14 patients with localized untreated prostate cancer for the purposes of digital gene expression profiling of CTCs, isolated using the new 3rd generation CTC iChip technology (6). Of these, 18 metastatic and 4 localized prostate cancer patients had detectable CTCs (Appendix, Fig. S1). Single CTCs were micromanipulated and processed for RNA sequencing and digital gene expression profiling, as described below.

Task 5. (Aim 2) Digital gene expression profiling of CTCs including sample preparation and RNA sequencing.

One of the goals of this Research Project is to identify cellular pathways that underlie the acquisition of treatment resistance in prostate cancer by dissecting the transcriptome of CTCs. In the previous reporting period, we demonstrated that the third generation CTC-chip technology (CTC-iChip) can be used to generate high purity CTC preparations in solution that can be micromanipulated for single cell analysis, enabling single cell whole transcriptome RNA-seq of CTCs from a mouse model of pancreatic cancer (7). We have now used similar techniques to isolate and sequence CTCs from blood acquired from human prostate cancer patients, as described in Task 4. This work was published in *Science* during this reporting period (8) (see Appendix).

Untagged and unfixed CTCs were identified by cell surface staining for epithelial (EpCAM) and mesenchymal (CDH11) markers and absent staining for the common leukocyte marker CD45. A total of 221 single candidate prostate CTCs were isolated from 18 patients with metastatic prostate cancer and 4 patients with localized prostate cancer (Appendix, Fig. S1). Of these, 133 cells (60%) had RNA of sufficient quality for amplification and next generation RNA sequencing, and 122 (55%) had >100,000 uniquely aligned sequencing reads (Appendix, Fig. S2A). In addition to candidate CTCs, we also obtained comprehensive transcriptomes for bulk primary prostate cancers from a separate cohort of 12 patients (macrodissected for >70% tumor content), 30 single cells derived from four different prostate cancer cell lines, and 5 patient-derived leukocyte controls. The leukocytes were readily distinguished by their expression of hematopoietic lineage markers and served to exclude any CTCs with potentially contaminating signals. Strict expression thresholds were used to define lineage-confirmed CTCs, scored by prostate lineage-specific genes (*PSA*, *PSMA*, *AMACR*, *AR*) and standard epithelial markers (*KRT7, KRT8*, *KRT18*, *KRT19*, *EPCAM*) (Appendix, Fig. S2B). Twenty-eight cells were excluded given the presence of leukocyte transcripts suggestive of cellular contamination or misidentification during selection, and 17 cells were excluded given low expression of both prostate lineage-specific genes and standard epithelial markers. The remaining 77 cells (from

13 patients; average of 6 CTCs per patient) were defined as lineage-confirmed CTCs (Appendix, Figs. S1 and S2).

Task 6. (Aim 2) Data analysis of CTC digital gene expression profiles.

During this reporting period, we completed analysis of the whole transcriptome digital gene expression profiles of the lineage-confirmed CTCs that were sequenced as described in Task 5. Unsupervised hierarchical clustering analysis of single prostate CTCs, primary tumor samples, and cancer cell lines resulted in their organization into distinct clusters (Appendix, Fig. 1A). Single CTCs from an individual patient showed considerably greater intercellular heterogeneity in their transcriptional profiles than single cells from prostate cancer cell lines (Appendix, Fig. 1, B and C; mean correlation coefficient 0.10 vs. 0.44, $P<1x10^{-20}$), but they strongly clustered according to patient of origin, indicating higher diversity in CTCs from different patients (Appendix, Fig. 1C and Fig. S2C; mean correlation coefficient 0.10 for CTCs within patient vs. 0.0014 for CTCs between patients, $P=2.0x10^{-11}$).

We performed differential gene expression analysis to identify genes that are upregulated in prostate CTCs compared to primary tumor samples. A total of 711 genes were highly expressed in CTCs compared to primary tumors, with the most enriched being the molecular chaperone *HSP90AA1*, which regulates the activation and stability of AR, among other functions (10), and the non-coding RNA transcript *MALAT1*, which has been implicated in alternative mRNA splicing and transcriptional control of gene expression (11) (Appendix, Fig. 2B and Fig. S4A; FDR<0.1 and fold-change >2). We used the Pathway Interaction Database (PID) (12) to identify key molecular pathways upregulated in CTCs versus primary tumors, as well as those upregulated in metastatic versus primary prostate tumors based on analyses of previously published datasets (Appendix, Fig. 2C and Fig. S5). In total, 21 pathways were specifically enriched in prostate CTCs, with the majority implicated in growth factor, cell adhesion, and hormone signaling (Appendix, Fig. 2D and Fig. S5).

We then performed retrospective differential analyses in subsets of CTCs to identify mechanisms of resistance to enzalutamide. From eight patients with metastatic prostate cancer who had not received enzalutamide (group A), 41 CTCs were compared with 36 CTCs from five patients whose cancer exhibited radiographic and/or PSA progression during therapy (group B) (Appendix, Fig. 3A and Table S1). Gene set enrichment analysis (GSEA) of candidate PID cellular signaling pathways showed significant enrichment for noncanonical Wnt signaling in group B compared with group A CTCs (Appendix, Fig. 3B and Fig. S6A; P=0.0064; FDR = 0.239). This signaling pathway, activated by a subset of Wnt ligands, mediates multiple downstream regulators of cell survival, proliferation, and motility (Appendix, Fig. S6B) (13). A separate analysis using a metagene for the PID non-canonical Wnt signature confirmed enrichment of the signature in group B compared with group A CTCs, at the level of both individual CTCs and individual patients (Appendix, Fig. 3A; P=0004 for CTCs). Among the downstream components of non-canonical Wnt, the most significantly enriched were *RAC1*, *RHOA*, and *CDC42*, signaling molecules involved in actin cytoskeleton and cell migration (Appendix, Fig. 3A and Fig. S6B).

Although most studies of CRPC have focused on acquired *AR* gene abnormalities, an alternative pathway, glucocorticoid receptor (GR) signaling, has recently been shown to contribute to anti-androgen resistance in a prostate cancer mouse xenograft model (14). Interestingly, we noted an inverse relationship in our human prostate CTC data set between *GR* expression and non-canonical Wnt signaling. Among CTCs with low *GR* expression, GSEA analysis showed significant enrichment for non-canonical Wnt signaling in enzalutamide-

progressing patients (group B) (P=0.025), which was absent in CTCs with high *GR* expression (P=0.34) (Appendix, Fig. 3B and Fig. S6D). Thus, these two AR-independent drug resistance pathways may predominate in different subsets of cancer cells.

Task 7. (Aim 2) Validation and follow-up studies of promising genes and pathways identified through CTC digital gene expression profiles.

During this reporting period, we have been engaged in validation studies in the laboratory based on genes and pathways implicated in disease progression and treatment resistance through our analysis of CTC transcriptional profiles described above. To test whether activation of non-canonical Wnt signaling modulates enzalutamide sensitivity, we ectopically expressed the non-canonical Wnt ligands *WNT4, WNT5A, WNT7B,* or *WNT11* in LNCaP androgen-sensitive prostate cancer cells, which express low endogenous levels (Appendix, Fig. S7A and S7B). Survival of the AR-positive LNCaP cells in the presence of enzalutamide was enhanced by the non-canonical Wnt ligands, particularly *WNT5A* (Appendix, Fig. 4A and Fig. S7C; $P=2.8 \times 10^{-5}$). Remarkably, endogenous *WNT5A* was acutely induced upon treatment with enzalutamide, suggestive of a feedback mechanism, and its depletion (knockdown) resulted in reduced cell proliferation (Appendix, Fig. 4B and Fig. S7D; $P=6.6 \times 10^{-4}$). We also generated stable enzalutamide-resistant LNCaP cells through prolonged in vitro selection (Appendix, Fig. S7E). These cells also exhibited increased expression of endogenous *WNT5A*, whose suppression reduced proliferation in enzalutamide-supplemented medium (Appendix, Fig. 4C and Fig. S7F). Finally, we tested the contribution of non-canonical Wnt signaling to antiandrogen resistance in an independent data set, interrogating a previously published mouse LNCaP xenograft model, in which aberrant activation of GR contributes to enzalutamide resistance (14). A significant association between enzalutamide resistance and non-canonical Wnt signaling was evident (P=0.023), which again showed an inverse relation between *GR* expression and non-canonical Wnt signaling (P=0.032 for *GR* low versus P=0.11 for *GR* high; Appendix, Fig. 4D and Fig. S8, A and B). This independent data set further validates the independent contributions of GR and non-canonical Wnt signaling to anti-androgen resistance.

Task 8. Preparation of results, presentations, and manuscripts.

This Research Project has thus far resulted in published manuscripts in *Cancer Discovery* (4), *Science Translational Medicine* (6), *Nature Reviews Clinical Oncology* (5), and *Cell Reports* (7). During this reporting period, an additional manuscript was published in *Science* describing our single cell RNA-sequencing whole transcriptome profiling of prostate CTCs, and our finding implicating the noncanonical Wnt signaling pathway in resistance to enzalutamide therapy (8). In addition, during this reporting period, the PI delivered several presentations at national and international meetings, including oral presentations at the American Society for Radiation Oncology Annual Meeting, the Chabner Colloquium sponsored by the Society for Translational Oncology, and the Global Summit on Genitourinary Malignancies. It is anticipated that several additional manuscripts will be published and additional presentations will be delivered during the remaining term of this Research Project.

Progress in Training Plan for PI.

This Physician Research Training Award combines a training plan for the PI consisting of mentorship, coursework, conferences, seminars, and patient care, together with an integrated research project to enable the PI to become an effective translational investigator in prostate cancer. During this reporting period, I have continued to attend regular formal mentorship meetings with Dr. Daniel Haber and Dr. Shyamala Maheswaran to discuss my research

progress and future research directions. I have also continued to meet with Dr. Matthew Smith on a regular basis for continued guidance regarding clinical aspects of my research. I have also continued to receive scientific guidance from key collaborators and advisors, including Dr. Mehmet Toner and Dr. Sridhar Ramaswamy.

With regard to coursework, conferences, and seminars, I have completed formal courses in clinical trial design, biostastistics, informed consent, and data safety and monitoring through the MGH Clinical Research Program Education Unit. During this reporting period, I attended regularly scheduled educational conferences, including the biweekly MGH multi-disciplinary urologic oncology conference, the MGH Cancer Center Grand Rounds, and the MGH Radiation Oncology chart rounds. I also attended the 2016 Annual Meeting of the American Association for Cancer Research (AACR) and the 2016 Annual American Society for Radiation Oncology (ASTRO) meeting.

Finally, as a component of my training as a physician scientist specialized in prostate cancer, I have continued to engage in the clinical care of patients as a radiation oncologist specializing in genitourinary malignancies. I have been devoting 1 day a week to the care of patients undergoing or who have completed radiation therapy, and a half day per week providing new consultations for patients presenting to the MGH Multidisciplinary GU Oncology clinic together with Urology and Medical Oncology colleagues. My clinical responsibilities have been limited to 20% to 30% of my total effort. Together, this training plan has been effective in enabling my growth as a translational prostate cancer investigator.

In recognition of my potential to be a successful independent investigator in translational prostate cancer research, I have been promoted to the position of Assistant Professor of Radiation Oncology at Harvard Medical School and Assistant Radiation Oncologist at the Massachusetts General Hospital.

KEY RESEARCH ACCOMPLISHMENTS

- Development of an androgen receptor (AR) signaling assay in CTCs based on a two-color PSA/PSMA immunofluorescence assay.
- Demonstration of the ability of the immunofluorescence-based AR signaling assay to measure AR activity in CTCs in patients with prostate cancer, and potentially predict patient outcomes after abiraterone acetate treatment.
- Development of a methodology to isolate single CTCs for RNA analysis using the microfluidic CTC-iChip.
- Demonstration of the feasibility of microfluidic qRT-PCR to measure mRNA transcript levels in single prostate CTCs.
- Demonstration of feasibility of RNA-sequencing and digital gene expression profiling of whole transcriptomes in single prostate CTCs.
- Successful RNA-sequencing of single prostate CTCs.
- Analysis of genes and pathways upregulated in CTCs compared to metastatic and primary tumors in patients with prostate cancer.
- Identification of the noncanonical Wnt signaling pathway as a potential mechanism of resistance to antiandrogen therapy in prostate cancer.

CONCLUSION

This Research Project uses a novel microfluidic technology called the “CTC-chip” to interrogate cellular signaling activity in circulating tumor cells (CTCs) isolated from metastatic prostate cancer patients in an effort to monitor and predict treatment response, as well as gain a deeper understanding of molecular mechanisms of treatment resistance (5, 9). An AR activity signature developed in prostate cancer cell lines is being applied to CTCs in patients with castration-resistant prostate cancer (CRPC) before and after secondary hormonal therapy to test the hypothesis that effective suppression of AR signaling in CTCs correlates with clinical response to hormonal therapy. To identify novel genes and pathways involved in the evolution of castration-resistant prostate cancer, single cell RNA-seq and digital gene expression profiling of CTCs is being performed. Thus far, this Research Project has successfully provided initial validation of novel molecular biomarkers that can monitor and predict responses to second-line hormonal therapy in patients with CRPC, as well as reveal fundamental insights into the mechanisms underlying castration-resistance in prostate cancer. Finally, this Award has enabled the protection of time for research and mentored training of the PI to continue his development towards a productive career as an independent investigator in translational prostate cancer research.

PUBLICATIONS, ABSTRACTS, AND PRESENTATIONS

- Manuscripts during this reporting period:

    - Peer-Reviewed Scientific Journals:
        - **Miyamoto, D.T.**, Zheng, Y., Wittner, B.S., Lee, R.J., Zhu, H., Broderick, K.T., Desai, R., Fox, D.B., Brannigan, B.W., Trautwein, J., Arora, K.S., Desai, N., Dahl, D.M., Sequist, L.V., Smith, M.R., Kapur, R., Wu, C.L., Shioda, T., Ramaswamy, S., Ting, D.T., Toner, M., Maheswaran, S., Haber, D.A. RNA-Seq of single prostate CTCs implicates noncanonical Wnt signaling in antiandrogen resistance. *Science* 2015; 349:1351-1356. PMID: 26383955

    - Abstracts:
        - **Miyamoto, D.T.**, Zheng, Y., Wittner, B.S., Lee, R.J., Zhu, H., Broderick, K.T., Desai, R., Brannigan, B.W., Arora, K.S., Dahl, D.M., Sequist, L.V., Smith, M.R., Kapur, R., Wu, C.L., Shioda, T., Ramaswamy, S., Ting, D.T., Toner, M., Maheswaran, S., Haber, D.A. (October, 2015). Single cell RNA profiling of circulating tumor cells in patients with prostate cancer. 2015 American Society for Radiation Oncology Annual Meeting, San Antonio, TX. (Oral Presentation).

- Presentations during this reporting period:

    - National:
        - **Miyamoto, D.T.** "Single cell RNA profiling of circulating tumor cells in patients with prostate cancer." Oral Presentation, American Society for Radiation Oncology 57th Annual Meeting, San Antonio, TX, October, 2015.
        - **Miyamoto, D.T.** "Molecular Analysis of CTCs in Prostate Cancer." Invited Lecture, Society for Translational Oncology, 2015 Chabner Colloquium, Boston, MA, October, 2015.
        - **Miyamoto, D.T.** "Molecular Profiling of Circulating Tumor Cells in Prostate Cancer." Invited Lecture, USC Norris Cancer Center Grand Rounds, University of Southern California, Los Angeles, CA, October, 2015.

    - International:
        - **Miyamoto, D.T.** "RNA-Seq of single prostate CTCs implicates noncanonical Wnt signaling in antiandrogen resistance." Global Summit on Genitourinary Malignancies, Banff Springs, Canada, October, 2015.

INVENTIONS, PATENTS, AND LICENSES

Nothing to report during this reporting period.

REPORTABLE OUTCOMES

- Androgen receptor (AR) signaling assay in CTCs based on a two-color PSA/PSMA immunofluorescence assay.
- Methodology to isolate single CTCs for RNA analysis using the microfluidic CTC-iChip.
- Identification of the noncanonical Wnt signaling pathway as involved in resistance to antiandrogen therapy.

OTHER ACHIEVEMENTS

The PI was promoted to Assistant Professor of Radiation Oncology at Harvard Medical School in June 2015 and Assistant Radiation Oncologist at the Massachusetts General Hospital in September 2015 based in part on accomplishments supported by this Award.

The PI received a Young Investigator Award from the Prostate Cancer Foundation in June of 2016.

REFERENCES

1. Chen Y, Clegg NJ, Scher HI. Anti-androgens and androgen-depleting therapies in prostate cancer: new agents for an established target. Lancet Oncol 2009; 10: 981-91.
2. de Bono JS, Logothetis CJ, Molina A, Fizazi K, North S, Chu L, et al. Abiraterone and increased survival in metastatic prostate cancer. N Engl J Med 2011; 364: 1995-2005.
3. Scher HI, Fizazi K, Saad F, Taplin ME, Sternberg CN, Miller K, et al. Increased survival with enzalutamide in prostate cancer after chemotherapy. N Engl J Med 2012; 367: 1187-97.
4. Miyamoto DT, Lee RJ, Stott SL, Ting DT, Wittner BS, Ulman M, et al. Androgen receptor signaling in circulating tumor cells as a marker of hormonally responsive prostate cancer. Cancer Discov 2012; 2: 995-1003.
5. Miyamoto DT, Sequist LV, Lee RJ. Circulating tumour cells-monitoring treatment response in prostate cancer. Nat Rev Clin Oncol 2014; 11: 401-12.
6. Ozkumur E, Shah AM, Ciciliano JC, Emmink BL, Miyamoto DT, Brachtel E, et al. Inertial focusing for tumor antigen-dependent and -independent sorting of rare circulating tumor cells. Sci Transl Med 2013; 5: 179ra47.
7. Ting DT, Wittner BS, Ligorio M, Vincent Jordan N, Shah AM, Miyamoto DT, et al. Single-Cell RNA Sequencing Identifies Extracellular Matrix Gene Expression by Pancreatic Circulating Tumor Cells. Cell reports 2014; 8: 1905-18.
8. Miyamoto DT, Zheng Y, Wittner BS, Lee RJ, Zhu H, Broderick KT, et al. RNA-Seq of single prostate CTCs implicates noncanonical Wnt signaling in antiandrogen resistance. Science 2015; 349: 1351-6.

9. Stott SL, Hsu CH, Tsukrov DI, Yu M, Miyamoto DT, Waltman BA, et al. Isolation of circulating tumor cells using a microvortex-generating herringbone-chip. Proc Natl Acad Sci U S A 2010; 107: 18392-7.
10. Trepel J, Mollapour M, Giaccone G, Neckers L. Targeting the dynamic HSP90 complex in cancer. Nat Rev Cancer 2010; 10: 537-49.
11. Gutschner T, Hammerle M, Diederichs S. MALAT1 -- a paradigm for long noncoding RNA function in cancer. Journal of molecular medicine 2013; 91: 791-801.
12. Schaefer CF, Anthony K, Krupa S, Buchoff J, Day M, Hannay T, et al. PID: the Pathway Interaction Database. Nucleic Acids Res 2009; 37: D674-9.
13. Katoh M, Katoh M. WNT signaling pathway and stem cell signaling network. Clin Cancer Res 2007; 13: 4042-5.
14. Arora VK, Schenkein E, Murali R, Subudhi SK, Wongvipat J, Balbas MD, et al. Glucocorticoid receptor confers resistance to antiandrogens by bypassing androgen receptor blockade. Cell 2013; 155: 1309-22.

APPENDICES

Includes the following: **Page**

Biosketch, David T. Miyamoto, July 2016 ..... **15**

Miyamoto et al. RNA-Seq of single prostate CTCs implicates noncanonical Wnt signaling in antiandrogen resistance. *Science*, 2015;349:1351-56 ..... **20**

Supplementary Materials for Miyamoto et al. RNA-Seq of single prostate CTCs implicates noncanonical Wnt signaling in antiandrogen resistance. *Science*, 2015;349:1351-56 ..... **26**

BIOGRAPHICAL SKETCH

Provide the following information for the Senior/key personnel and other significant contributors.
Follow this format for each person. DO NOT EXCEED FIVE PAGES.

NAME: Miyamoto, David T.

eRA COMMONS USER NAME (credential, e.g., agency login): DMIYAMOTO

POSITION TITLE: Assistant Professor of Radiation Oncology, Harvard Medical School, Assistant Radiation Oncologist, Massachusetts General Hospital

EDUCATION/TRAINING *(Begin with baccalaureate or other initial professional education, such as nursing, include postdoctoral training and residency training if applicable. Add/delete rows as necessary.)*

INSTITUTION AND LOCATION	DEGREE *(if applicable)*	Completion Date MM/YYYY	FIELD OF STUDY
Harvard College, Cambridge, MA	A.B.	06/1997	Chemistry
Harvard University, Cambridge, MA	Ph.D.	11/2004	Cell & Developmental Biology
Harvard Medical School, Boston, MA	M.D.	06/2006	Medicine
Brigham & Women's Hospital, Boston, MA	Intern	06/2007	Internal Medicine
Harvard Radiation Oncology Program, Boston, MA	Resident	06/2011	Radiation Oncology
Massachusetts General Hospital Cancer Center / Howard Hughes Medical Institute	Postdoctoral	06/2015	Cancer Genetics

A. Personal Statement

My multidisciplinary training in molecular cell biology, clinical radiation oncology, and cancer biology has enabled me to become a translational physician scientist with a strong clinical and research interest in genitourinary malignancies. I received my MD-PhD working in the laboratory of Dr. Timothy Mitchison studying the mechanisms of cell division. My postdoctoral research involved the study of circulating tumor cells (CTCs) in prostate cancer with Dr. Daniel Haber. I am now an Assistant Professor of Radiation Oncology at Harvard Medical School, devoting 80% of my effort to translational cancer research and 20% to clinical activities treating patients with genitourinary malignancies. My research focuses on the development of novel biomarkers to guide the treatment of patients with genitourinary malignancies, including microfluidic technologies for the detection and molecular analysis of CTCs.

1. **Miyamoto, D.T.**, Zheng, Y., Wittner, B.S., Lee, R.J., Zhu, H., Broderick, K.T., Desai, R., Fox, D.B., Brannigan, B.W., Trautwein, J., Arora, K.S., Desai, N., Dahl, D.M., Sequist, L.V., Smith, M.R., Kapur, R., Wu, C.L., Shioda, T., Ramaswamy, S., Ting, D.T., Toner, M., Maheswaran, S., Haber, D.A. (2015). RNA-Seq of single prostate CTCs implicates noncanonical Wnt signaling in antiandrogen resistance. *Science*, 349:1351-1356.
2. **Miyamoto, D.T.,** Lee, R.J., Stott, S.L., Ting, D.T., Wittner, B.S., Ulman, M., Smas, M.E., Lord, J.B., Brannigan, B.W., Trautwein, J., Bander, N.H., Wu, C.L., Sequist, L.V., Smith, M.R., Ramaswamy, S., Toner, M., Maheswaran, S., Haber, D.A., Androgen receptor signaling in circulating tumor cells as a marker of hormonally responsive prostate cancer. *Cancer Discovery*, 2012 Nov;2:995-1003. PMCID:PMC3508523
3. **Miyamoto, D.T.**, Sequist, L.V., Lee, R.J. (2014). Circulating tumour cells – monitoring treatment response in prostate cancer. *Nature Reviews Clinical Oncology*, 11(7):401-12.

4. Aceto, N., Bardia, A., **Miyamoto, D.T.**, Donaldson, M.C., Wittner, B.S., Spencer, J.A., Yu, M., Pely, A., Engstrom, A., Zhu, H., Brannigan, B.W., Kapur, R., Stott, S.L., Shioda, T., Ramaswamy, S., Ting, D.T., Lin, C.P., Toner, M., Haber, D.A., Maheswaran, S. (2014). Circulating tumor cell clusters are oligoclonal precursors of breast cancer metastasis. *Cell*, 158:1110-1122. PMCID:PMC4149753

B. Positions and Honors

Positions and Employment

2011 - 2015	Instructor in Radiation Oncology, Harvard Medical School, Boston, MA
2011 - 2015	Assistant in Radiation Oncology, Massachusetts General Hospital, Boston, MA
2015 -	Assistant Professor of Radiation Oncology, Harvard Medical School, Boston, MA
2015 -	Assistant Radiation Oncologist, Massachusetts General Hospital, Boston, MA

Other Professional Positions

1999 - 2006	Resident Tutor in Medicine, Leverett House, Harvard College, Cambridge, MA
2007	Visiting Physician, National Cancer Center Hospital, Tokyo, Japan
2011 -	Harvard-MIT Health Sciences and Technology MD Board of Advisors, Harvard Medical School

Honors

1993	National Merit Scholarship
1993 – 1997	John Harvard Scholarship
1996	Merck Undergraduate Research Fellow
1997	*Magna cum laude*, Harvard College
1997	High Honors in Chemistry, Harvard College
2001 – 2004	Howard Hughes Medical Institute Predoctoral Fellow
2009 – 2011	B. Leonard Holman Research Pathway, American Board of Radiology
2010	ASTRO Annual Meeting Scientific Abstract Award
2011 – 2013	A. David Mazzone Career Development Award, Dana-Farber/Harvard Cancer Center
2011 – 2012	Research Career Development Award, Federal Share of the Proton Beam, NCI/MGH
2012	Ira J. Spiro Translational Research Award
2012 – 2017	Physician Research Training Award, Department of Defense
2014	Ira J. Spiro Translational Research Award
2016	Prostate Cancer Foundation Young Investigator Award

Licensure and Certification

2008 – present	Massachusetts Full License, Board of Registration in Medicine
2012 – present	Board Certification, Radiation Oncology, American Board of Radiology

Membership in Professional Societies

2013 – present	Member, American Association for Cancer Research
2008 – present	Member, American Society for Radiation Oncology
2003 – present	Member, American Society for Cell Biology
2008 – 2011	Member, Radiological Society of North America
2009 – 2011	Member, American Society of Clinical Oncology

C. Contribution to Science

1. My early publications focused on the elucidation of fundamental mechanisms underlying mitotic spindle assembly and function. Proper function of the mitotic spindle is necessary for the faithful segregation of chromosomes during cell division, and components of this dynamic macromolecular structure may serve as potential targets for cancer therapy. I served as the primary investigator or co-investigator in all of these studies.

a. **Miyamoto, D.T.**, Perlman, Z.E., Burbank, K.S., Groen, A.C., and Mitchison, T.J. (2004). The kinesin Eg5 drives poleward microtubule flux in *Xenopus* egg extract spindles. *The Journal of Cell Biology*, 167:813-8. PMCID:PMC2172449
b. Haggarty, S.J., Mayer, T.U., **Miyamoto, D.T.**, Fathi, R., King, R.W., Mitchison, T.J., and Schreiber, S.L. (2000). Dissecting cellular processes using small molecules: identification of colchicine-, taxol-like, and other small molecules that perturb mitosis. *Chemistry & Biology*, 7:275-86.
c. Groen, A.C., Cameron, L.A., Coughlin, M., **Miyamoto, D.T.**, Mitchison, T.J., and Ohi, R. (2004). XRHAMM functions in Ran-dependent microtubule nucleation and pole formation during anastral spindle assembly. *Current Biology*, 14:1801-11.
d. **Miyamoto, D.T.**, Perlman, Z.E., Mitchison, T.J., and Shirasu-Hiza, M. (2003). Dynamics of the mitotic spindle – potential therapeutic targets. In: Meijer, L., Jezequel, A., and Roberge, M., editors. *Progress in Cell Cycle Research*, Volume 5. New York: Plenum Press; p. 349-60.

2. Development of novel microfluidic platforms for the isolation of circulating tumor cells from patients.

Circulating tumor cells (CTCs) are rare cancer cells shed from primary and metastatic tumors into the peripheral blood, and represent a "liquid biopsy" that may be performed repeatedly and non-invasively to study tumor evolution during therapy. However, given their rarity, estimated at 1 cell per billion blood cells, they are extremely difficult to isolate. In collaboration with Dr. Daniel Haber, Dr. Mehmet Toner, and colleagues, I have played an integral role in the development of microfluidic technologies to efficiently isolate CTCs from the peripheral blood of patients. I developed a series of immunofluorescence assays to quantitate prostate CTCs isolated using the microfluidic CTC-chip platform, and used this assay to develop the capabilities of the 2nd generation (^{HB}CTC-Chip) (Stott et al. *PNAS* 2010) and the 3rd generation CTC isolation technologies (CTC-iChip) (Ozkumur et al. *Science Translational Medicine* 2013). I used the ^{HB}CTC-Chip to demonstrate the presence of clusters of CTCs in selected metastatic prostate cancer patients (Stott et al. *PNAS* 2010). Most recently, we have developed a specialized microfluidic device to specifically capture these CTC clusters, thus enabling the further study of their unique biology. I served as co-investigator in all of these studies.

a. Stott, S.L., Hsu, C.H., Tsukrov, D., Yu, M., **Miyamoto, D.T.**, Waltman, B.A., Rothenberg, S.M., Shah, A.M., Smas, M.E., Korir, G., Floyd, F.P., Gilman, A., Lord, J.B., Winokur, D., Nagrath, S., Sequist, L.V., Lee, R.J., Isselbacher, K.J., Maheswaran, S., Haber, D.A., Toner, M. (2010). Isolation of circulating tumor cells using a microvortex-generating herringbone-chip. *Proceedings of the National Academy of Sciences U.S.A.*, 107:18392-7. PMCID:PMC2972993.
b. Ozkumur, E., Shah, A.M., Ciciliano, J.C., Emmink, B.L., **Miyamoto, D.T.**, Brachtel, E., Yu, M., Chen, P., Morgan, B., Trautwein, J., Kimura, A., Sengupta, S., Stott, S.L., Karabacak, N.M., Barber, T.A., Walsh, J.R., Smith, K., Spuhler, P., Sullivan, J., Lee, R., Ting, D.T., Luo, X., Shaw, A.T., Bardia, A., Sequist, L.V., Louis, D.N., Maheswaran, S., Kapur, R., Haber, D.A., Toner, M. (2013). Inertial Focusing for Positive and Negative Sorting of Rare Circulating Tumor Cells. *Science Translational Medicine*, 5:179ra47. PMCID:PMC3760275.
c. Sarioglu, A.F., Aceto, N., Kojic, N., Donaldson, M.C., Zeinali, M., Hamza, B., Engstrom, A., Zhu, H., Sundarasen, T.K., **Miyamoto, D.T.**, Luo, X., Bardia, A., Wittner, B., Ramaswamy, S., Shioda, T., Ting, D.T., Stott, S.L., Kapur, R., Maheswaran, S., Haber, D., Toner, M. (2015). A microfluidic device for label-free, physical capture of circulating tumor cell-clusters. *Nature Methods*, 12:685-91. PMCID:PMC4490017.

3. CTC-based assays to monitor and predict treatment responses in prostate cancer patients.

Circulating tumor cells (CTCs) represent a means of performing noninvasive tumor sampling, and may enable the monitoring and prediction of treatment response in patients with prostate cancer. I have developed a quantitative immunofluorescence assay to accurately measure androgen receptor (AR) signaling activity status in CTCs from patients with prostate cancer, which can monitor real-time changes in AR activity in response to AR-targeting therapies. The assay also can predict treatment responses prior to initiation of therapy, and thus may be instrumental in the rational application of second generation anti-androgen therapies (Miyamoto et al.

Cancer Discovery 2012; cover article). We are currently validating these findings in a prospective clinical trial (DF/HCC 03-209). I am also co-inventor on a patent based on this assay (U.S. Patent Application 61/667,040, filed July 2, 2012). In addition, I have measured changes in CTC numbers after surgical resection of localized prostate cancer (Stott et al. *Science Translational Medicine* 2010), and I am leading an effort to investigate the role of CTC analysis in early stage prostate cancer. I have had the opportunity to provide perspective on the state of the prostate CTC field in a recent review (Miyamoto et al. *Nature Reviews Clinical Oncology* 2014).

a. **Miyamoto, D.T.,** Lee, R.J., Stott, S.L., Ting, D.T., Wittner, B.S., Ulman, M., Smas, M.E., Lord, J.B., Brannigan, B.W., Trautwein, J., Bander, N.H., Wu, C.L., Sequist, L.V., Smith, M.R., Ramaswamy, S., Toner, M., Maheswaran, S., Haber, D.A. (2012). Androgen receptor signaling in circulating tumor cells as a marker of hormonally responsive prostate cancer. *Cancer Discovery*, 2:995-1003. PMCID:PMC3508523
b. Stott, S.L., Lee, R.J., Nagrath, S., Yu, M., **Miyamoto, D.T.**, Ulkus, L., Inserra, E.J., Ulman, M., Springer, S., Nakamura, Z., Moore, A.L., Tsukrov, D.I., Kempner, M.E., Dahl, D.M., Wu, C., Iafrate, A.J., Smith, M.R., Tompkins, R.G., Sequist, L.V., Toner, M., Haber, D.A., Maheswaran, S. (2010). Microfluidic isolation and molecular characterization of circulating tumor cells from patients with localized and metastatic prostate cancer. *Science Translational Medicine*, 2:25ra23:1-10.PMCID:PMC3141292.
c. **Miyamoto, D.T.**, Sequist, L.V., Lee, R.J. (2014). Circulating tumour cells – monitoring treatment response in prostate cancer. *Nature Reviews Clinical Oncology*, 11(7):401-12.

4. Development of robust single cell sequencing methods for the isolation and molecular analysis of single CTCs, to study heterogeneity and mechanisms of treatment resistance.

Although the CTC-iChip enables the highly efficient enrichment of CTCs from whole blood, the resultant CTC product is a mixture of bulk CTCs combined with contaminating leukocytes. To enable the detailed molecular characterization of 100% pure single CTCs, I established a robust methodology for the staining, visualization, micromanipulation, and molecular characterization of individual CTCs following CTC-iChip processing. I used this method to provide the first demonstration of microfluidic qRT-PCR of single human CTCs isolated using the CTC-iChip (Ozkumur et al. *Science Translational Medicine* 2013). We have also used these methods to perform single cell RNA-seq of CTCs isolated from a mouse model of pancreatic cancer (Ting et al. *Cell Reports* 2014), and to perform RNA-seq of single CTCs and clusters of CTCs from patients with breast cancer (Aceto et al. *Cell* 2014). Most recently, I have successfully accomplished single cell RNA-seq analysis on a series of CTCs isolated from patients with prostate cancer (Miyamoto et al. *Science* 2015).

a. **Miyamoto, D.T.**, Zheng, Y., Wittner, B.S., Lee, R.J., Zhu, H., Broderick, K.T., Desai, R., Fox, D.B., Brannigan, B.W., Trautwein, J., Arora, K.S., Desai, N., Dahl, D.M., Sequist, L.V., Smith, M.R., Kapur, R., Wu, C.L., Shioda, T., Ramaswamy, S., Ting, D.T., Toner, M., Maheswaran, S., Haber, D.A. (2015). RNA-Seq of single prostate CTCs implicates noncanonical Wnt signaling in antiandrogen resistance. *Science*, 349:1351-1356.
b. Aceto, N., Bardia, A., **Miyamoto, D.T.**, Donaldson, M.C., Wittner, B.S., Spencer, J.A., Yu, M., Pely, A., Engstrom, A., Zhu, H., Brannigan, B.W., Kapur, R., Stott, S.L., Shioda, T., Ramaswamy, S., Ting, D.T., Lin, C.P., Toner, M., Haber, D.A., Maheswaran, S. (2014). Circulating tumor cell clusters are oligoclonal precursors of breast cancer metastasis. *Cell*, 158:1110-1122. PMCID:PMC4149753.
c. Ting, D.T., Wittner, B.S., Ligorio, M., Vincent Jordan, N., Shah, A.M., **Miyamoto, D.T.**, Aceto, N., Bersani, F., Brannigan, B.W., Xega, K., Ciciliano, J.C., Zhu, H., MacKenzie, O.C., Trautwein, J., Arora, K.S., Shahid, M., Ellis, H.L., Qu, N., Bardeesy, N., Rivera, M.N., Deshpande, V., Ferrone, C.R., Kapur, R., Ramaswamy, S., Shioda, T., Toner, M., Maheswaran, S., Haber, D.A. Single-cell RNA sequencing identifies extracellular matrix gene expression by pancreatic circulating tumor cells. *Cell Reports* 2014; 8:1905-18. PMCID:PMC4230325.

Complete List of Published Work in MyBibliography:
http://www.ncbi.nlm.nih.gov/sites/myncbi/1vG7CpGOY8jQt/bibliograpahy/45002366/public/?sort=date&direction=descending

D. Research Support

Ongoing Research Support

Department of Defense — Miyamoto (PI) — 07/01/2012 – 06/30/2017
Physician Research Training Award, Prostate Cancer Research Program
Probing androgen receptor signaling in circulating tumor cells in prostate cancer.
The main goals of this project are to define an AR activity score in CTCs and test the hypothesis that AR signaling activity in prostate CTCs correlates with response to second-line hormonal therapy in metastatic prostate cancer patients and to perform digital gene expression (DGE) profiling of prostate CTCs to identify novel pathways that promote castration resistance.

NCI/MGH
Federal Share of the Proton Beam Program, Spiro Award — Miyamoto (PI) — 04/15/2014 – 10/14/2016
Discovery of Genomic Classifiers for Prediction of Response to Bladder Sparing Therapy for Muscle-Invasive Bladder Cancer
The main goals of this project is the discovery of genomic-based classifiers (GC) and genomic-clinical-based classifiers (GCC) as predictive models for response to CMT for patients diagnosed with invasive bladder cancer who underwent Maximal TURBT procedure, using paraffin embedded TURBT specimens. Also the evaluation of GC in comparison with and in combination with existing biomarkers and nomograms (*4*). Correlation of GC with clinicopathologic subcategories, and evaluation of predictive power for bladder-intact survival, disease-specific survival, and overall survival.

C06 CA 059267 — Hong/Efstathiou (Co-PIs) — 10/1/2004 – 12/31/2019
NCI Federal Share Program Income
Proton Biospecimen & Biomarker Program
The major goal of this project is to establishment a Proton Biomarker Program (PBP) at MGH, which will provide necessary research tissue banking resources and consolidate biomarker research efforts for more effective incorporation of biomarker exploration in clinical trials at MGH and beyond. Role: Co-Investigator

C06 CA059267 — Efstathiou (PI) — 01/01/12-12/31/16
NCI Federal Share Program Income
Phase III Randomized Clinical Trial of Proton Therapy vs. IMRT for Low or Intermediate Risk Prostate Cancer
The main goals of this project are to assess the clinical and cost effectiveness of PBT versus IMRT for men with low or intermediate risk prostate cancer. Role: Co-Investigator

Completed Research Support

Howard Hughes Medical Institute Predoctoral Fellowship — Miyamoto (PI) — 07/01/2001-11/30/2004
Probing the functions of kinesins in mitosis.

NCI/MGH — Miyamoto (PI) — 07/01/2011-06/30/2012
Federal Share of the Proton Beam Program, Research Career Development Award
Molecular characterization of circulating tumor cells in prostate cancer.

Dana Farber/Harvard Cancer Center — Miyamoto (PI) — 08/01/2011-08/31/2013
A. David Mazzone Career Development Award
Probing androgen receptor signaling in circulating tumor cells in prostate cancer.

NCI/MGH
Federal Share of the Proton Beam Program, Spiro Award — Miyamoto (PI) — 04/15/2012 – 10/14/2014
Evaluation of Multigene Expression Signatures as Predictors of Outcome After Radiation Therapy for Prostate Cancer

Overlap

None

PROSTATE CANCER

RNA-Seq of single prostate CTCs implicates noncanonical Wnt signaling in antiandrogen resistance

David T. Miyamoto,[1,2*] Yu Zheng,[1,3*] Ben S. Wittner,[1,4] Richard J. Lee,[1,4] Huili Zhu,[1] Katherine T. Broderick,[1] Rushil Desai,[1] Douglas B. Fox,[1] Brian W. Brannigan,[1] Julie Trautwein,[1] Kshitij S. Arora,[1,5] Niyati Desai,[1,5] Douglas M. Dahl,[1,6] Lecia V. Sequist,[1,4] Matthew R. Smith,[1,4] Ravi Kapur,[7] Chin-Lee Wu,[1,5] Toshi Shioda,[1] Sridhar Ramaswamy,[1,4] David T. Ting,[1,4] Mehmet Toner,[7] Shyamala Maheswaran,[1,8]† Daniel A. Haber[1,3,4]†

Prostate cancer is initially responsive to androgen deprivation, but the effectiveness of androgen receptor (AR) inhibitors in recurrent disease is variable. Biopsy of bone metastases is challenging; hence, sampling circulating tumor cells (CTCs) may reveal drug-resistance mechanisms. We established single-cell RNA-sequencing (RNA-Seq) profiles of 77 intact CTCs isolated from 13 patients (mean six CTCs per patient), by using microfluidic enrichment. Single CTCs from each individual display considerable heterogeneity, including expression of *AR* gene mutations and splicing variants. Retrospective analysis of CTCs from patients progressing under treatment with an AR inhibitor, compared with untreated cases, indicates activation of noncanonical Wnt signaling ($P = 0.0064$). Ectopic expression of Wnt5a in prostate cancer cells attenuates the antiproliferative effect of AR inhibition, whereas its suppression in drug-resistant cells restores partial sensitivity, a correlation also evident in an established mouse model. Thus, single-cell analysis of prostate CTCs reveals heterogeneity in signaling pathways that could contribute to treatment failure.

After the initial response of metastatic prostate cancer to androgen deprivation therapy (ADT), it invariably recurs as castration-resistant disease (*1*). Second-line inhibitors of the androgen receptor (AR) have been shown to increase overall survival in castration-resistant prostate cancer (CRPC), consistent with the reactivation of AR signaling in the tumor, but responses are heterogeneous and often short-lived, and resistance to therapy is a pressing clinical problem (*1*). In other types of cancer, molecular analyses of serial biopsies have enabled the study of acquired drug-resistance mechanisms, intratumor heterogeneity, and tumor evolution in response to therapy (*2*)—an approach that is restricted by the predominance of bone metastases in prostate cancer (*3*, *4*). Thus, isolation of circulating tumor cells (CTCs) may enable noninvasive monitoring, as patients initially respond and subsequently become refractory to therapies targeting the AR pathway (*5*). Here, we established single-cell RNA-sequencing (RNA-Seq) profiles of CTCs, individually isolated after microfluidic enrichment from blood specimens of men with prostate cancer, to address their heterogeneity within and across different patients and their differences from primary tumor specimens. Retrospective analyses of clinical and molecular data were then performed to identify potentially clinically relevant mechanisms of acquired drug resistance.

Building on earlier approaches for capturing and scoring CTCs (*3*), highly efficient microfluidic technologies enable molecular analyses (*6*–*9*). We applied the CTC-iChip to magnetically deplete normal hematopoietic cells from whole-blood specimens (*10*). Untagged and unfixed CTCs were identified by cell surface staining for epithelial and mesenchymal markers [epithelial cell adhesion molecule (EpCAM) and cadherin-11 (CDH11), respectively], and absent staining for the common leukocyte marker CD45. These labeled CTCs were then individually micromanipulated (fig. S1, A and B). A total of 221 single-candidate prostate CTCs were isolated from 18 patients with metastatic prostate cancer and 4 patients with localized prostate cancer (fig. S1C and table S1). Of these, 133 cells (60%) had RNA of sufficient quality for amplification and next-generation RNA sequencing, and 122 (55%) had >100,000 uniquely aligned sequencing reads (*11*) (figs. S1C and S2A). Although many cancer cells in the circulation appear to undergo apoptosis, the presence of intact RNA identifies the subset enriched for viable cells. In addition to candidate CTCs, we also obtained comprehensive transcriptomes for bulk primary prostate cancers from a separate cohort of 12 patients (macrodissected for >70% tumor content) (table S2), 30 single cells derived from four different prostate cancer cell lines, and five patient-derived leukocyte controls (fig. S1C). The leukocytes were readily distinguished by their expression of hematopoietic lineage markers and served to exclude any CTCs with potentially contaminating signals. Strict expression thresholds were used to define lineage-confirmed CTCs, scored by prostate lineage-specific genes (*PSA*, *PSMA*, *AMACR*, and *AR*) and standard epithelial markers (*KRT7*, *KRT8*, *KRT18*, *KRT19*, and *EPCAM*) (*11*) (fig. S2B). Given the presence of leukocyte transcripts suggestive of cellular contamination or misidentification during selection, 28 cells were excluded, and, given low expression of both prostate lineage-specific genes and standard epithelial markers, 17 cells were excluded. The remaining 77 cells (from 13 patients; average of six CTCs per patient) were defined as categorical CTCs (fig. S1C and table S1).

Unsupervised hierarchical clustering analysis of single prostate CTCs, primary tumor samples, and cancer cell lines resulted in their organization into distinct clusters (Fig. 1A). Single CTCs from an individual patient showed considerably greater intercellular heterogeneity in their transcriptional profiles than single cells from prostate cancer cell lines (Fig. 1, B and C) (mean correlation coefficient 0.10 versus 0.44, $P < 1 \times 10^{-20}$), but they strongly clustered according to patient of origin, which indicated higher diversity in CTCs from different patients (Fig. 1C and fig. S2C) (mean correlation coefficient 0.10 for CTCs within patient versus 0.0014 for CTCs between patients, $P = 2.0 \times 10^{-11}$).

We examined gene markers of prostate lineage, epithelial, mesenchymal, and stem cell fates, and cellular proliferation (Fig. 2A). Epithelial markers were abundantly expressed [>10 reads per million (rpm)] by nearly all CTCs analyzed (92%), whereas mesenchymal genes were not up-regulated compared with primary tumors or prostate cancer–derived cell lines. Among robustly expressed transcripts were putative stem cell markers (*12*), including *ALDH7A1*, *CD44*, and *KLF4*, present in 60% of CTCs. In addition, 47% of CTCs expressed markers of cell proliferation. We performed differential gene expression analysis to identify genes that are up-regulated in prostate CTCs compared with primary tumor samples. A total of 711 genes were highly expressed in CTCs compared with primary tumors; the most enriched were (i) the molecular chaperone *HSP90AA1*, which regulates the activation and stability of AR, among other functions (*13*), and (ii) the non-coding RNA transcript *MALAT1*, which has been implicated in alternative mRNA splicing and transcriptional control of gene expression (*14*) (Fig. 2B, fig. S4A, and table S3) [false discovery rate (FDR) < 0.1, and fold change > 2]. We used the Pathway Interaction Database (PID) (*15*) to identify key molecular pathways up-regulated in

[1]Massachusetts General Cancer Center, Massachusetts General Hospital, Harvard Medical School, Charlestown, MA 02129, USA. [2]Department of Radiation Oncology, Massachusetts General Hospital, Harvard Medical School, Charlestown, MA 02129, USA. [3]Howard Hughes Medical Institute, Chevy Chase, MD 20815, USA. [4]Department of Medicine, Massachusetts General Hospital, Harvard Medical School, Charlestown, MA 02129, USA. [5]Department of Pathology, Massachusetts General Hospital, Harvard Medical School, Charlestown, MA 02129, USA. [6]Department of Urology, Massachusetts General Hospital, Harvard Medical School, Charlestown, MA 02129, USA. [7]Center for Bioengineering in Medicine, Massachusetts General Hospital, Harvard Medical School, Charlestown, MA 02129, USA. [8]Department of Surgery, Massachusetts General Hospital, Harvard Medical School, Charlestown, MA 02129, USA.
*These authors contributed equally to this work. †Corresponding author. E-mail: haber@helix.mgh.harvard.edu (D.H.); smaheswaran@mgh.harvard.edu (S.M.)

CTCs versus primary tumors, as well as those upregulated in metastatic versus primary prostate tumors, on the basis of analyses of previously published data sets (*11*) (Fig. 2C, fig. S5, and table S4). In total, 21 pathways were specifically enriched in prostate CTCs, with the majority implicated in growth factor, cell adhesion, and hormone signaling (Fig. 2D and fig. S5).

The AR pathway constitutes the primary therapeutic target in prostate cancer, with specific mutations in *AR* (*1*, *16*) and *AR* mRNA splice variants (*17*, *18*) implicated in acquired resistance. The *AR* transcript was expressed (>10 rpm) in 60 out of 77 (78%) CTCs (12 out of 13 patients with prostate cancer). The T877A mutation (Thr^{877} replaced by Ala) in AR, previously associated with ligand promiscuity and resistance to antiandrogens (*1*), was identified in five out of nine CTCs from a single (1 out of 13) patient with metastatic CRPC (Fig. 3A and table S5). The F876L mutation (Phe^{876} replaced by Leu) in the ligand-binding domain, which converts the AR antagonist enzalutamide to a potential AR agonist (*19*, *20*), was not detected in any of the CTCs (<1 out of 32 CTCs with sufficient sequencing reads for mutational analysis). Thus, in our study, point mutations in *AR* known to be associated with altered signaling were uncommon in patients with CRPC, consistent with other reports (*4*, *21*).

We then analyzed *AR* mRNA splice variants lacking a ligand-binding domain and encoding constitutively active proteins (*1*, *17*). These alternative transcripts are not attributable to discrete genetic mutations, but they are commonly expressed in CRPC (*4*), and detection in bulk CTC preparations of the single splice variant *AR-V7* has been correlated to clinical resistance to antiandrogens (*18*). Our single-cell analysis revealed far more complex and heterogeneous patterns of *AR* splice-variant expression among individual CTCs from patients with CRPC: 33 out of 73 (43%) expressed at least one type of *AR* splice variant (8 out of 11 CRPC patients). Among these CTCs, 26 out of 73 (36%) expressed *AR-V7* (8 out of 11 patients); 18 out of 73 (25%) had a distinct splice form *ARv567es* (*AR-V12*) (8 out of 11 patients); and 7 out of 73 (10%) had *AR-V1*, *AR-V3*, or *AR-V4* splice variants (5 out of 11 patients), all of which are known to result in altered signaling (Fig. 3A and table S6). Simultaneous expression of more than one type of *AR* splice variant was observed in 13 out of 73 (18%) single CTCs (7 out of 11 patients). In total, 7 out of 11 (64%) CRPC patients had CTCs with more than one type of *AR* alteration (including *AR* splice variants and point mutations). In contrast, no such alterations were evident in 12 primary prostate tumors, and only one out of four CTCs from two patients with castration-sensitive prostate cancer (CSPC) that was previously untreated had low-level expression of the *AR-V7* splice variant (Fig. 3A and table S6). Aberrant alternative splicing is a recognized feature of many cancers (*22*), and indeed, another prostate-specific transcript, *KLK3* (*PSA*) (*23*), showed many more alternative splice variants in CTCs from metastatic patients compared with primary tumors (P = 0.0088) (fig. S4B). Taken together, our observations indicate that intrapatient tumor heterogeneity is such that individual CTCs may have different or multiple mRNA splicing alterations.

Tumor heterogeneity is thought to increase further as second-line therapies exert additional selective pressure. We performed retrospective differential analyses in subsets of CTCs to identify mechanisms of resistance to enzalutamide, a potent AR inhibitor recently approved by the U.S. Food and Drug Administration for CRPC (*24*). From eight patients with metastatic prostate cancer who had not received enzalutamide (group A), 41 CTCs were compared with 36 CTCs from five patients whose cancer exhibited radiographic and/or prostate-specific antigen (PSA) progression during therapy (group B) (Fig. 3A and table S1). Gene set enrichment analysis (GSEA) of candidate PID cellular signaling pathways showed significant enrichment for noncanonical Wnt signaling in group B compared with group A CTCs

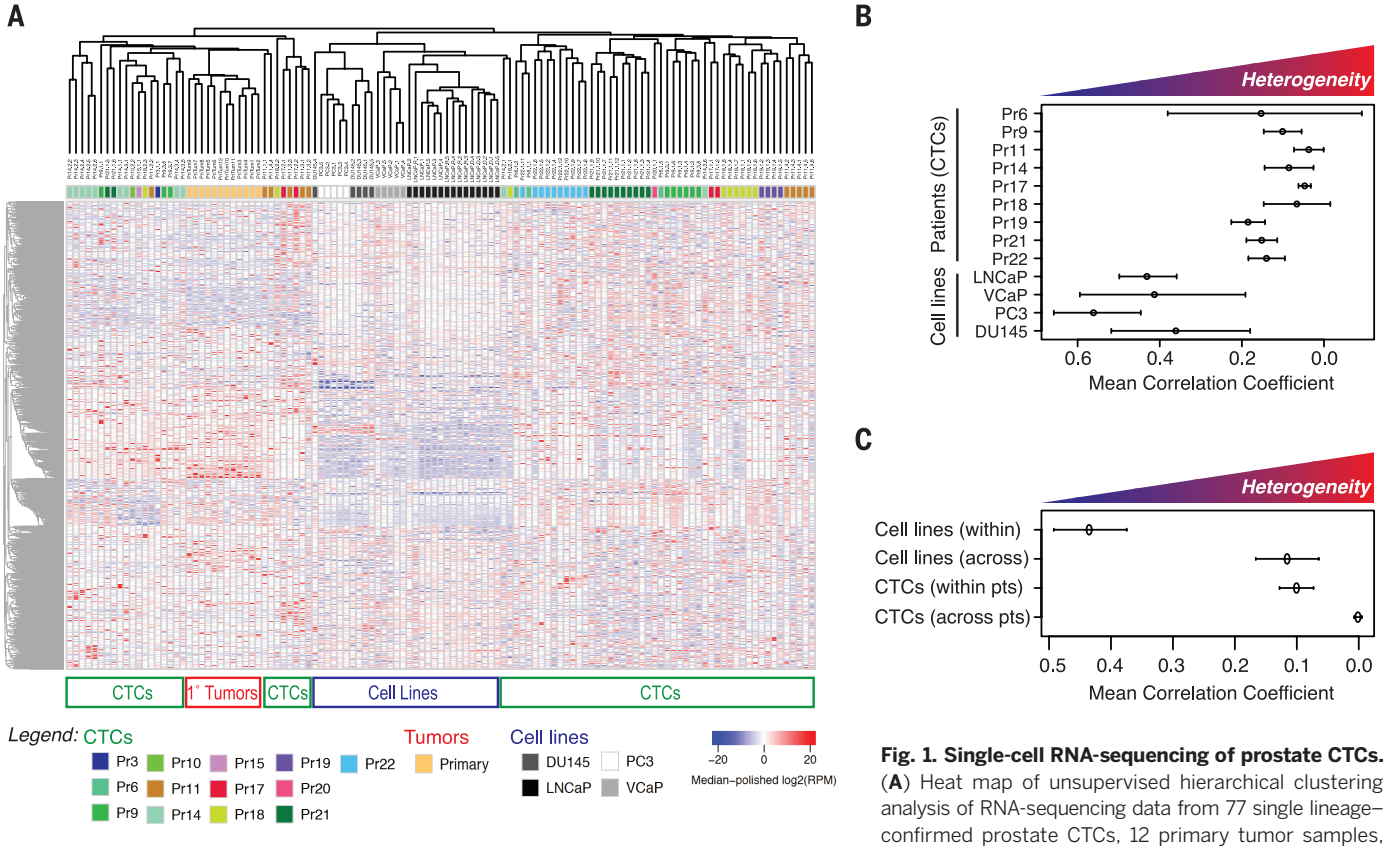

Fig. 1. Single-cell RNA-sequencing of prostate CTCs. (**A**) Heat map of unsupervised hierarchical clustering analysis of RNA-sequencing data from 77 single lineage–confirmed prostate CTCs, 12 primary tumor samples, and 30 single cells from four prostate cancer cell lines. (**B**) Heterogeneity, measured by mean correlation coefficient within individual samples with three or more cells available for analysis. (**C**) Heterogeneity analysis showing mean correlation coefficients from expression data for CTCs between and within patients (0.0013838 versus 0.10055; Holm corrected $P = 2.0 \times 10^{-11}$), and for prostate cancer cell lines between and within lines (0.11568 versus 0.43534; Holm corrected $P = 5.42 \times 10^{-14}$).

(Fig. 3B and fig. S6A) (P = 0.0064; FDR = 0.239). This signaling pathway, activated by a subset of Wnt ligands, mediates multiple downstream regulators of cell survival, proliferation, and motility (fig. S6B) (*25*–*28*). A separate analysis using a metagene for the PID noncanonical Wnt signature (*11*) (table S7) confirmed enrichment of the signature in group B compared with group A CTCs, at the level of both individual CTCs and individual patients (Fig. 3A) [P = 0.0041 (CTCs); P = 0.04 (patients)]. Among the downstream components of noncanonical Wnt, the most significantly enriched were *RAC1*, *RHOA*, and *CDC42*, signaling molecules involved in actin cytoskeleton remodeling and cell migration (Fig. 3A and fig. S6B) [$P = 1 \times 10^{-6}$ (*RAC1*), P = 0.0046 (*RHOA*), P = 0.0097 (*CDC42*)]. In contrast, *AR* abnormalities were not significantly increased among either individual CTCs or patients, when comparing enzalutamide-resistant versus enzalutamide-naïve cases, using a similar analysis (Fig. 3A).

Although most studies of CRPC have focused on acquired *AR* gene abnormalities, an alternative pathway, glucocorticoid receptor (GR) signaling, has recently been shown to contribute to antiandrogen resistance in a prostate cancer mouse xenograft model (*29*). Within our human prostate CTC data set, *GR* transcripts and a metagene signature of GR signaling (*11*) (table S7) did not reach statistical significance between patients in group A versus B [P = 0.35 (CTCs); P = 0.59 (patients)] (Fig. 3A), but an inverse relationship between *GR* expression and noncanonical Wnt signaling was evident. Among CTCs with low *GR* expression, GSEA analysis showed significant enrichment for noncanonical Wnt signaling in

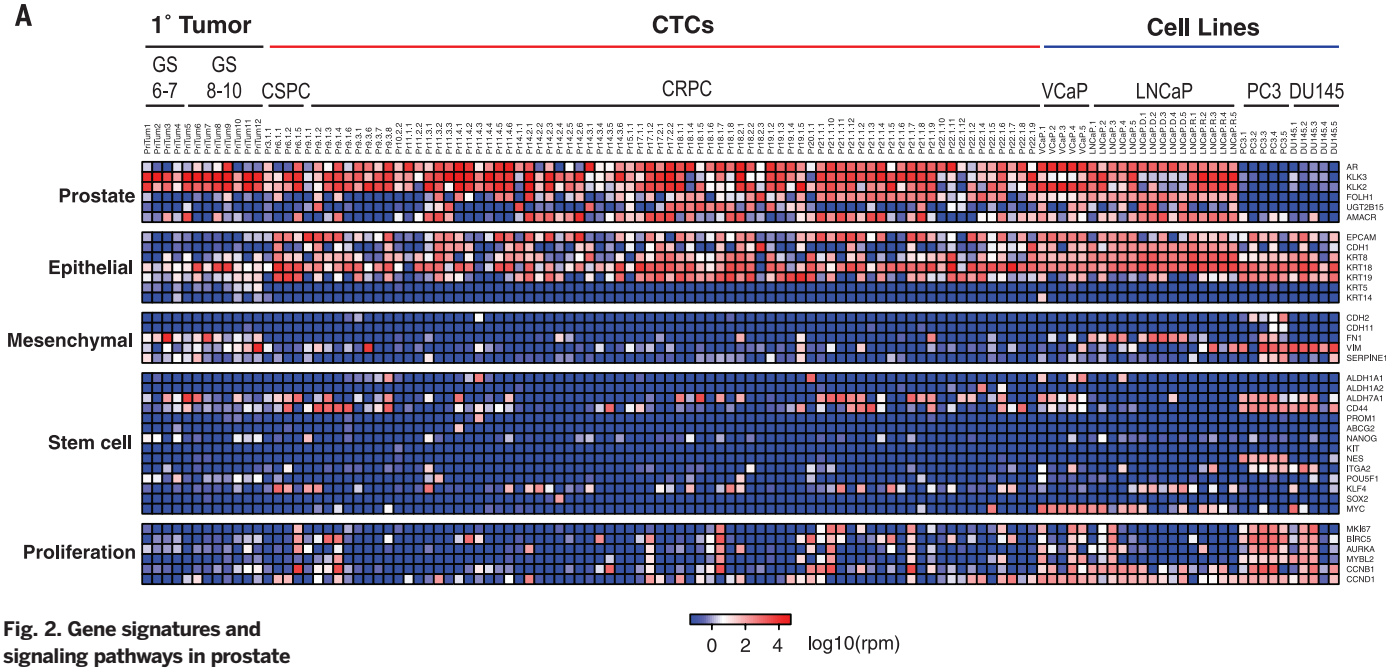

Fig. 2. Gene signatures and signaling pathways in prostate CTCs. (**A**) High-resolution heat map showing expression of selected gene panels in single prostate CTCs, primary tumor samples, and prostate cancer cell lines. GS, Gleason score; VCaP, a PSA-producing cell line; LNCaP.R, LNCaP cells treated with R1881; LNCaP.D, LNCaP cells treated with dimethyl sulfoxide as a vehicle control. (**B**) Genes differentially expressed by prostate CTCs and primary prostate tumors (FDR < 0.1, and fold change > 2). (**C**) PID molecular pathways (*15*) enriched in CTCs compared with primary tumors and in metastases compared with primary tumors (based on analysis of multiple data sets; see fig. S5 and table S4). (**D**) Signaling pathways enriched in prostate CTCs. Molecular pathways from the PID up-regulated in CTCs versus primary tumors (excluding those enriched in metastases compared with primary tumors), organized by PID categorization (*15*) (fig. S5). Abbreviations (other than proteins, clockwise from top): HDAC, histone deacetylase; AJ, adherens junction; IL2 and IL3, interleukins; ERBB1, epidermal growth factor receptor B1; TGFBR, transforming growth factor-β receptor.

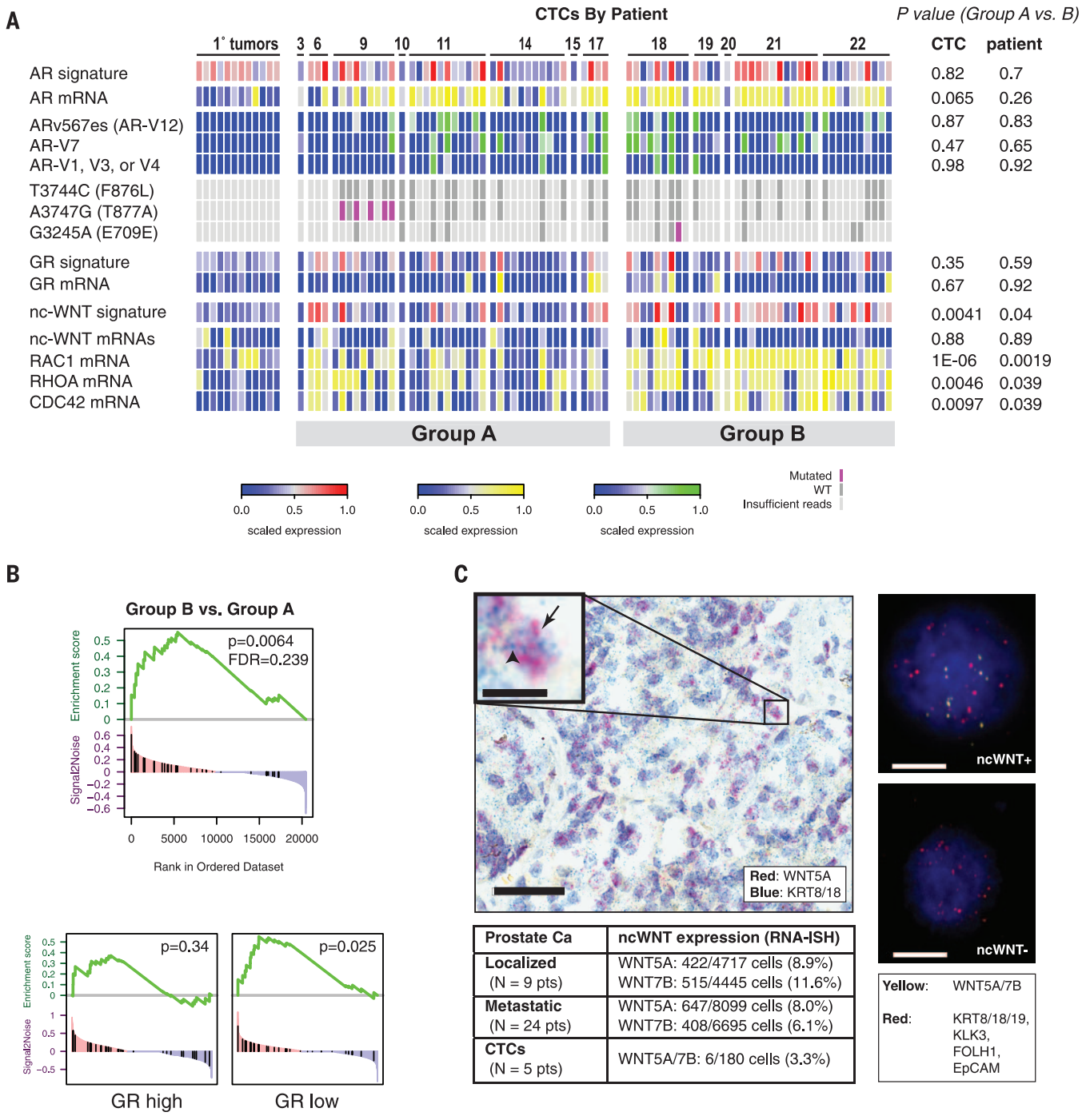

Prostate Ca	ncWNT expression (RNA-ISH)
Localized (N = 9 pts)	WNT5A: 422/4717 cells (8.9%) WNT7B: 515/4445 cells (11.6%)
Metastatic (N = 24 pts)	WNT5A: 647/8099 cells (8.0%) WNT7B: 408/6695 cells (6.1%)
CTCs (N = 5 pts)	WNT5A/7B: 6/180 cells (3.3%)

Fig. 3. Heterogeneity of treatment resistance mechanisms in prostate CTCs. (**A**) Heat map depicting androgen receptor (AR) abnormalities, selected signaling pathway signatures, and genes in radical prostatectomy specimens, prostate CTCs from enzalutamide-naïve patients (group A), and prostate CTCs from patients who had radiographic or biochemical progression of disease while receiving treatment with enzalutamide (group B). Noncanonical Wnt signature is from reference (*15*), glucocorticoid receptor (GR) signature is from reference (*29*), and AR signature is from reference (*32*) (table S7). Numbers at top of heat map represent ID numbers (Pr numbers) for patients from which each CTC is derived. (**B**) (Top) GSEA plots showing enrichment of noncanonical Wnt (nc-Wnt) pathway in CTCs from group B (patients with cancer progression on enzalutamide) compared with group A (enzalutamide-naïve patients). (Bottom) Enrichment of noncanonical Wnt pathway in CTCs from group B compared with group A, stratified by GR gene expression. (**C**) (Left) Representative micrograph (40×) of RNA-in situ hybridization assay in metastatic prostate tumors, probing for *WNT5A* and *KRT8/18*, scale bar, 50 μm. (Inset) High magnification, arrow points to *WNT5A* signal (red dot), arrowhead points to *KRT8/18* signal (blue dot), scale bar, 10 μm. Adjacent tissue sections were probed for *WNT7B*, and quantification of RNA-ISH data are displayed in the table. Of nine primary tumors examined, five had >1% WNT5A expression in KRT+ cells (range 0.3%-42%) and seven had >1% WNT7B expression (range 0.5%-33.6%). Of 24 metastatic tumors examined, 16 had >1% WNT5A expression (range 0 to 50.5%) and 15 had >1% WNT7B expression (range 0 to 26%). (Right) Representative fluorescence micrographs of RNA in situ hybridization in prostate CTCs, probing for *WNT5A/7B* (yellow dots), and prostate CTC-specific markers (*EPCAM*, *KLK3*, *FOLH1*, *KRT8/18/19*) (red dots). DNA is stained with 4′,6′-diamidino-2-phenylindole (blue). Scale bar, 10 μm.

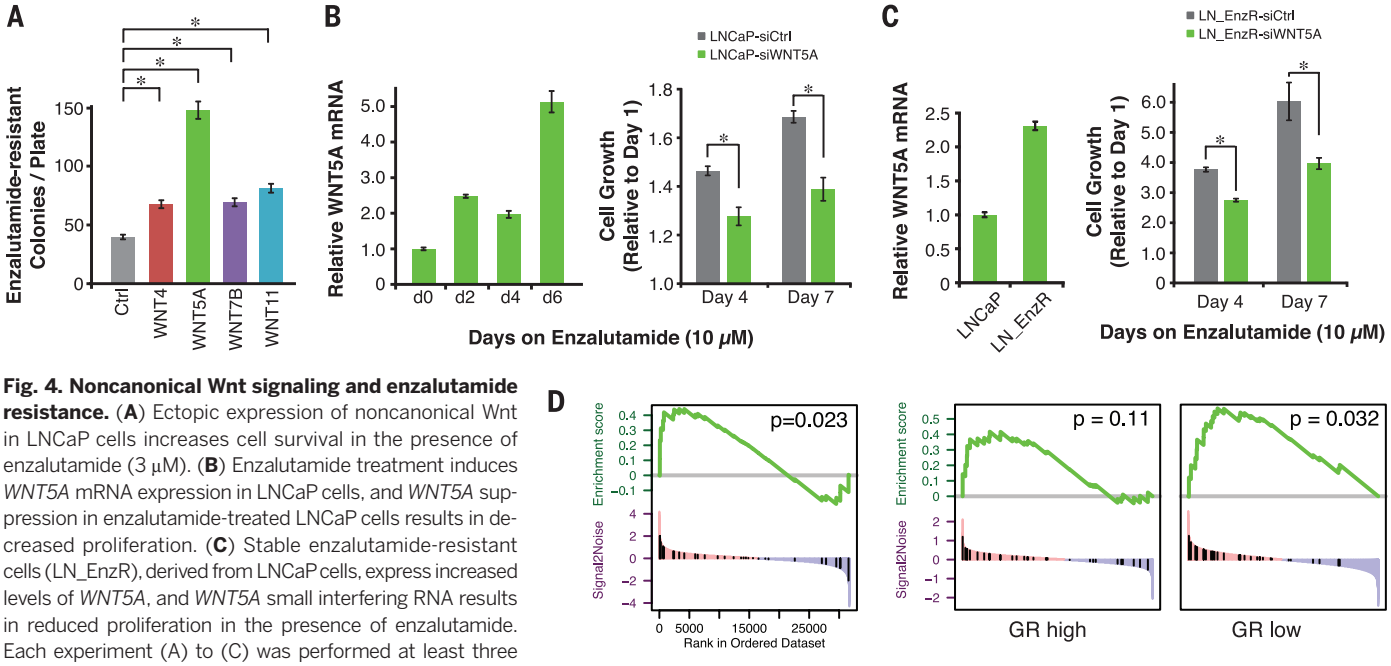

Fig. 4. Noncanonical Wnt signaling and enzalutamide resistance. (**A**) Ectopic expression of noncanonical Wnt in LNCaP cells increases cell survival in the presence of enzalutamide (3 μM). (**B**) Enzalutamide treatment induces *WNT5A* mRNA expression in LNCaP cells, and *WNT5A* suppression in enzalutamide-treated LNCaP cells results in decreased proliferation. (**C**) Stable enzalutamide-resistant cells (LN_EnzR), derived from LNCaP cells, express increased levels of *WNT5A*, and *WNT5A* small interfering RNA results in reduced proliferation in the presence of enzalutamide. Each experiment (A) to (C) was performed at least three times. Data are presented as means ± SD. (**D**) (Left) GSEA plot showing enrichment of noncanonical Wnt pathway in mouse xenografts derived from enzalutamide-resistant LREX′ cells (*29*) compared with control xenografts derived from LNCaP/AR cells (data from LREX′ and Con B entries, GEO GSE52169). (Right) GSEA plots showing noncanonical Wnt pathway enrichment in antiandrogen-resistant xenografts, when stratified by GR gene expression (data from Res and Con A entries, GEO GSE52169).

enzalutamide-progressing patients (group B) (P = 0.025), which was absent in CTCs with high *GR* expression (P = 0.34) (Fig. 3B and fig. S6D). Thus, these two AR-independent drug resistance pathways may predominate in different subsets of cancer cells.

Wnt proteins may be secreted by tumor cells as part of an autocrine loop, or they may be produced by surrounding stromal cells. We used RNA in situ hybridization (RNA-ISH) to identify the source of WNT production in tumor specimens and CTCs. Within primary untreated prostate cancers (n = 9), the noncanonical *WNT5A* and *WNT7B* mRNAs were present in a subset of tumor cells (8.9 and 11.6%, respectively), but both were rare in surrounding stromal cells (<0.2 and 0.5%, respectively) (Fig. 3C and fig. S6C). Metastatic tumor biopsies from patients with CRPC (n = 24) also had readily detectable *WNT5A* and *WNT7B* (8.0 and 6.1%, respectively) (Fig. 3C). Similarly, *WNT5A* or *WNT7B* mRNA was detected by RNA-ISH in a subset of CTCs from patients (n = 5) with CRPC (6 out of 180 CTCs; 3.3%) (Fig. 3C). Thus, a subset of prostate cancer cells express noncanonical Wnt ligands, which may provide survival signals in the context of AR inhibition.

To test whether activation of noncanonical Wnt signaling modulates enzalutamide sensitivity, we ectopically expressed the noncanonical ligands *WNT4*, *WNT5A*, *WNT7B*, or *WNT11* in LNCaP androgen-sensitive human prostate cancer cells, which express low endogenous levels (fig. S7, A and B). Survival of the AR-positive LNCaP cells in the presence of enzalutamide was enhanced by the noncanonical Wnt ligands, particularly *WNT5A* (Fig. 4A) ($P = 2.8 \times 10^{-5}$) (fig. S7C). Remarkably, endogenous *WNT5A* was acutely induced upon treatment with enzalutamide, suggestive of a feedback mechanism, and its depletion (knockdown) resulted in reduced cell proliferation (Fig. 4B and fig. S7D) ($P = 6.6 \times 10^{-4}$). We also generated stable enzalutamide-resistant LNCaP cells through prolonged in vitro selection (fig. S7E). These cells also exhibited increased expression of endogenous *WNT5A*, whose suppression reduced proliferation in enzalutamide-supplemented medium (Fig. 4C) (P = 0.005) (fig. S7F). Finally, we tested the contribution of noncanonical Wnt to antiandrogen resistance in an independent data set, interrogating the previously published mouse LNCaP xenograft model, in which aberrant activation of GR contributes to enzalutamide resistance (*29*). A significant association between enzalutamide resistance and noncanonical Wnt signaling was evident (P = 0.023), which again showed an inverse relation between *GR* expression and noncanonical Wnt signaling (P = 0.032 for *GR* low versus P = 0.11 for *GR* high) (Fig. 4D and fig. S8, A and B). This independent data set further validates the independent contributions of GR and noncanonical Wnt signaling to antiandrogen resistance.

In summary, by RNA profiling single prostate CTCs, we demonstrate their differences from primary tumors, as well as their heterogeneity within individual patients. The acquisition of AR-dependent and AR-independent alterations conferring resistance to antiandrogen therapies is also heterogeneous. Among *AR* alterations, more than half of all patients had multiple *AR* splice variants present within different CTCs and about 1 out of 6 of single cancer cells had simultaneous expression of several *AR* splice variants. Two AR-independent pathways, activation of GR and noncanonical Wnt signaling, coexist in different subsets of cells. Wnt signaling has been implicated in multiple cellular functions linked to prostate cancer progression (*4*, *25*–*28*), and noncanonical Wnt signaling may be targeted by suppression of its key downstream components, such as Rho kinase (*30*). Our study is limited by its retrospective nature and relatively small sample size (13 patients; average of six CTCs per patient), a consequence of the rarity of intact CTCs and inefficiencies inherent in manual single-cell micromanipulation techniques, obstacles that might be overcome with future improvements in CTC isolation and single-cell sequencing technologies. Nevertheless, the heterogeneity of CTCs in patients with CRPC stands in contrast to the striking homogeneity of AR signaling in single CTCs from untreated patients (*5*). Although these observations require validation in prospective trials, they point to complex and heterogeneous drug resistance mechanisms in advanced prostate cancer, which may affect therapeutic efficacy.

REFERENCES AND NOTES

1. A. Egan *et al.*, *Cancer Treat. Rev.* **40**, 426–433 (2014).
2. M. Gerlinger *et al.*, *N. Engl. J. Med.* **366**, 883–892 (2012).
3. H. I. Scher, M. J. Morris, S. Larson, G. Heller, *Nat. Rev. Clin. Oncol.* **10**, 225–234 (2013).
4. D. Robinson *et al.*, *Cell* **161**, 1215–1228 (2015).
5. D. T. Miyamoto *et al.*, *Cancer Discov* **2**, 995–1003 (2012).
6. D. Ramsköld *et al.*, *Nat. Biotechnol.* **30**, 777–782 (2012).
7. J. G. Lohr *et al.*, *Nat. Biotechnol.* **32**, 479–484 (2014).
8. N. Aceto *et al.*, *Cell* **158**, 1110–1122 (2014).
9. D. T. Ting *et al.*, *Cell Reports* **8**, 1905–1918 (2014).
10. E. Ozkumur *et al.*, *Sci. Transl. Med.* **5**, 179ra47 (2013).
11. Materials and methods are available as supporting material on *Science* Online.

12. B. Sharpe, M. Beresford, R. Bowen, J. Mitchard, A. D. Chalmers, *Stem Cell Rev.* **9**, 721–730 (2013).
13. J. Trepel, M. Mollapour, G. Giaccone, L. Neckers, *Nat. Rev. Cancer* **10**, 537–549 (2010).
14. T. Gutschner, M. Hämmerle, S. Diederichs, *J. Mol. Med. (Berlin)* **91**, 791–801 (2013).
15. C. F. Schaefer *et al.*, *Nucleic Acids Res.* **37** (Database), D674–D679 (2009).
16. B. Gottlieb, L. K. Beitel, A. Nadarajah, M. Paliouras, M. Trifiro, *Hum. Mutat.* **33**, 887–894 (2012).
17. C. Lu, J. Luo, *Transl. Androl. Urol.* **2**, 178–186 (2013).
18. E. S. Antonarakis *et al.*, *N. Engl. J. Med.* **371**, 1028–1038 (2014).
19. M. D. Balbas *et al.*, *eLife* **2**, e00499 (2013).
20. J. D. Joseph *et al.*, *Cancer Discov* **3**, 1020–1029 (2013).
21. S. Carreira *et al.*, *Sci. Transl. Med.* **6**, 254ra125 (2014).
22. J. Zhang, J. L. Manley, *Cancer Discov* **3**, 1228–1237 (2013).
23. L. Kurlender *et al.*, *Biochim. Biophys. Acta* **1755**, 1–14 (2005).
24. H. I. Scher *et al.*, *N. Engl. J. Med.* **367**, 1187–1197 (2012).
25. M. Katoh, M. Katoh, *Clin. Cancer Res.* **13**, 4042–4045 (2007).
26. S. Takahashi *et al.*, *Proc. Natl. Acad. Sci. U.S.A.* **108**, 4938–4943 (2011).
27. D. Zheng *et al.*, *Mol. Cancer Res.* **11**, 482–493 (2013).
28. T. S. Gujral *et al.*, *Cell* **159**, 844–856 (2014).
29. V. K. Arora *et al.*, *Cell* **155**, 1309–1322 (2013).
30. N. Rath, M. F. Olson, *EMBO Rep.* **13**, 900–908 (2012).
31. F. Tang *et al.*, *Nat. Methods* **6**, 377–382 (2009).
32. H. Hieronymus *et al.*, *Cancer Cell* **10**, 321–330 (2006).

ACKNOWLEDGMENTS

We thank C. Sawyers for helpful discussions; A. McGovern, E. Stadtmueller, and B. Abebe for clinical trial support; and L. Libby and L. Nieman for technical assistance. This work was supported by grants from the Prostate Cancer Foundation (D.A.H., S.M., M.T., M.R.S., and R.J.L.), Charles Evans Foundation (D.A.H.), Department of Defense (D.T.M., R.J.L., and D.T.T.), Stand Up to Cancer (D.A.H., M.T., S.M., and L.V.S.), Howard Hughes Medical Institute (D.A.H.), National Institute of Biomedical Imaging and Bioengineering (NIBIB), NIH, EB008047 (M.T.), NCI 2RO1CA129933 (D.A.H.), National Cancer Institute, NCI, Federal Share Program and Income (S.M. and D.T.M.), Affymetrix, Inc. (D.T.T., K.A., and N.D.), Mazzone Program–Dana-Farber Harvard Cancer Center (D.T.M.), Burroughs Wellcome Fund (D.T.T.), and the Massachusetts General Hospital–Johnson & Johnson Center for Excellence in CTC Technologies (D.A.H., M.T., and S.M.). D.T.T. is a paid consultant for Affymetrix, Inc.; R.J.L. is a paid consultant for Janssen LLC. The Massachusetts General Hospital has filed for patent protection for the CTC-iChip technology. RNA-sequencing data have been deposited in GEO under accession number GSE67980.

SUPPLEMENTARY MATERIALS

www.sciencemag.org/content/349/6254/1351/suppl/DC1
Materials and Methods
Figs. S1 to S8
Tables S1 to S7
References (*33*–*37*)

10 March 2015; accepted 3 August 2015
10.1126/science.aab0917

SMALL PEPTIDES

Pri sORF peptides induce selective proteasome-mediated protein processing

J. Zanet,[1,2]* E. Benrabah,[1,2]* T. Li,[3] A. Pélissier-Monier,[1,2] H. Chanut-Delalande,[1,2] B. Ronsin,[1,2] H. J. Bellen,[3,4] F. Payre,[1,2]† S. Plaza[1,2]†

A wide variety of RNAs encode small open-reading-frame (smORF/sORF) peptides, but their functions are largely unknown. Here, we show that *Drosophila polished-rice* (*pri*) sORF peptides trigger proteasome-mediated protein processing, converting the Shavenbaby (Svb) transcription repressor into a shorter activator. A genome-wide RNA interference screen identifies an E2-E3 ubiquitin-conjugating complex, UbcD6-Ubr3, which targets Svb to the proteasome in a *pri*-dependent manner. Upon interaction with Ubr3, Pri peptides promote the binding of Ubr3 to Svb. Ubr3 can then ubiquitinate the Svb N terminus, which is degraded by the proteasome. The C-terminal domains protect Svb from complete degradation and ensure appropriate processing. Our data show that Pri peptides control selectivity of Ubr3 binding, which suggests that the family of sORF peptides may contain an extended repertoire of protein regulators.

Eukaryotic genomes encode many noncoding RNAs (ncRNAs) that lack the classical hallmarks of protein-coding genes. However, both ncRNAs and mRNAs often contain small open reading frames (sORFs), and there is growing evidence that they can produce peptides, from yeast (*1*) to plants (*2*, *3*) or humans (*4*, *5*). The *polished rice* or *tarsal-less* (*pri*) RNA contains four sORFs that encode highly related 11– to 32–amino acid peptides, required for embryonic development across insect species (*6*–*8*). In flies, *pri* is essential for the differentiation of epidermal outgrowths called trichomes (*7*, *8*). Trichome development is governed by the Shavenbaby (Svb) transcription factor (*9*–*11*); however, only in the presence of *pri* can Svb turn on the program of trichome development, i.e., activate expression of cellular effectors (*12*, *13*). Indeed, the Svb protein is translated as a large repressor, *pri* then induces truncation of its N-terminal region, which leads to a shorter activator (*12*). Thereby, *pri* defines the developmental timing of epidermal differentiation, in a direct response to systemic ecdysone hormonal signaling (*14*). Although we now have a clear framework for the developmental functions of *pri*, how these small peptides can trigger Svb processing is unknown.

To identify factors required for Svb processing in response to *pri*, we performed a genome-wide RNA interference (RNAi) screen in a cell line co-expressing green fluorescent protein (GFP)–tagged Svb and *pri* (Fig. 1A). We set up an automated assay quantifying Svb processing for each of the *Drosophila* genes, with an inhibitory score reflecting the proportion of cells unable to cleave off the Svb N terminus (see the supplementary materials). *pri* RNAi displayed the highest score, which validated our approach to identifying molecular players in Svb processing. Methods used to evaluate results from genome-wide screening all converged on a key role for the proteasome. For instance, COMPLEAT, a bioinformatic frame-

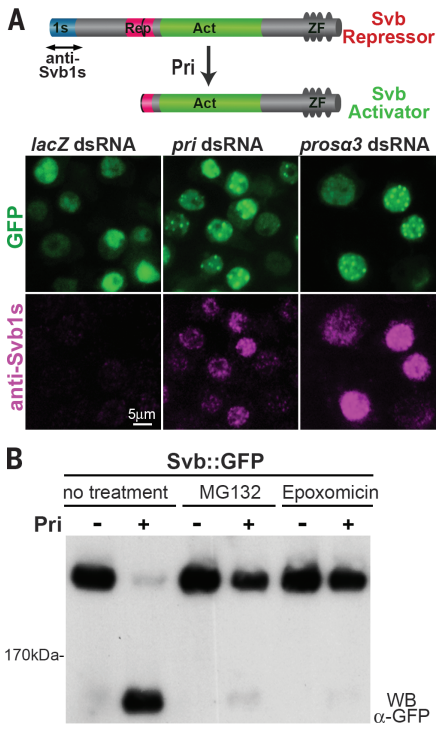

Fig. 1. Pri-dependent processing of Svb requires proteasome activity. (**A**) Drawing of Svb processing (antibody against Svb1s recognizes the repressor-specific N-terminal region) and snapshots from the screen illustrating the effect of double-stranded RNA against *lacZ* (negative control), *pri*, and *proteasomeα3* subunit (*prosα3*) on Svb::GFP processing. Cells were stained for Svb1s (purple) and GFP (green). (**B**) Western blot analysis of cells that express Svb::GFP, with or without *pri* and proteasome inhibitors (MG132, epoxomicin).

[1]Centre de Biologie du Développement, Université de Toulouse III—Paul Sabatier, Bâtiment 4R3, 118 route de Narbonne, F-31062 Toulouse, France. [2]CNRS, UMR5547, Centre de Biologie du Développement, F-31062 Toulouse, France. [3]Program in Developmental Biology, Baylor College of Medicine, Houston, TX 77030, USA. [4]Department of Molecular and Human Genetics, Howard Hughes Medical Institute, Neurological Research Institute, Baylor College of Medicine, Houston, TX 77030, USA.
*These authors contributed equally to this work. **†Corresponding author. E-mail: francois.payre@univ-tlse3.fr (F.P.); serge.plaza@univ-tlse3.f (S.P.)**

Originally posted 17 September 2015; revised 25 September 2015

www.sciencemag.org/content/349/6254/1351/suppl/DC1

Supplementary Materials for

RNA-Seq of single prostate CTCs implicates noncanonical Wnt signaling in antiandrogen resistance

David T. Miyamoto, Yu Zheng, Ben S. Wittner, Richard J. Lee, Huili Zhu, Katherine T. Broderick, Rushil Desai, Douglas B. Fox, Brian W. Brannigan, Julie Trautwein, Kshitij S. Arora, Niyati Desai, Douglas M. Dahl, Lecia V. Sequist, Matthew R. Smith, Ravi Kapur, Chin-Lee Wu, Toshi Shioda, Sridhar Ramaswamy, David T. Ting, Mehmet Toner, Shyamala Maheswaran,* Daniel A. Haber*

*Corresponding author. E-mail: haber@helix.mgh.harvard.edu (D.H.); smaheswaran@mgh.harvard.edu (S.M.)

Published 18 September 2015, *Science* **349**, 1351 (2015)
DOI: 10.1126/science.aab0917

This PDF file includes

Materials and Methods
Figs. S1 to S8
Tables S1 and S2
References

Other Supplementary Material for this manuscript includes the following:
(available at www.sciencemag.org/content/349/6254/1351/suppl/DC1)

Table S3. Genes differentially expressed between CTCs and primary prostate tumors.

Table S4. Data sets used in the differential gene expression and pathway analyses comparing metastatic and primary prostate tumors (see Figs. 2C and S5).

Table S5. Androgen receptor mutation analysis in prostate CTCs, primary tumors, and prostate cancer cell lines.

Table S6. Androgen receptor splice variant analysis in prostate CTCs and primary tumors.

Table S7. Pathway signatures used for metagene analyses in this study (see Fig. 3A).

Correction (25 September 2015): References were renumbered after the file was posted. The renumbering affected the supplementary reference citations, the list of references, and Table S7. The originally posted version can be seen here.

Materials and Methods

Patients and clinical specimens

Patients with a diagnosis of prostate cancer provided informed consent to one of two Institutional Review Board approved protocols (metastatic disease, (DF/HCC 05-300), or localized prostate cancer, (DF/HCC 08-207)). A total of 38 patients donated 20 mL of blood for CTC analysis, of which 18 patients with metastatic prostate cancer and 4 patients with localized untreated prostate cancer had identifiable CTCs (see below and Fig. S1C). Disease status and therapy at the time of CTC collection for each patient are provided in Table S1. Patients were retrospectively categorized as Group A if they had not received enzalutamide at the time of CTC collection (enzalutamide-naïve), and Group B if they were treated with enzalutamide at the time of CTC collection and their cancer exhibited radiographic and/or PSA progression during enzalutamide therapy. Frozen primary tumor tissues from an additional 12 patients with localized prostate cancer were sectioned, macrodissected for >70% tumor content, and subjected to RNA extraction, prior to diluting to single cell levels and processing for RNA sequencing (see below). Detailed patient characteristics are provided in Table S2. Additional frozen primary prostate tumors from 9 patients and metastatic tumors from 24 patients were obtained, sectioned, and processed for RNA-ISH (see below).

Circulating tumor cell isolation

Single CTCs were isolated from fresh whole blood following leukocyte depletion using the microfluidic CTC-iChip as previously described (*10*). To maximize recovery of intact CTCs with high quality RNA, blood samples were processed within 4 hours of being collected from the patient. The total time for single CTC isolation after receipt of fresh blood samples in the lab was approximately 2.5 hours. Briefly, whole blood samples were spiked with biotinylated antibodies against CD45 (R&D Systems, clone 2D1) and CD66 (AbD Serotec, clone 80H3), followed by incubation with Dynabeads MyOne Streptavidin T1 (Invitrogen) to achieve magnetic labeling and depletion of white blood cells. After processing of whole blood with the CTC-iChip, the CTC-enriched product was stained in solution with Alexa 488-conjugated antibodies against EpCAM (Cell Signaling Technology, clone VU1D9) and Cadherin 11 (CDH11) (R&D Systems, clone 667039) to identify CTCs, and PE-CF594-conjugated antibody against CD45 (BD Biosciences, clone HI30) to counterstain contaminating leukocytes. Patient blood samples were screened by microscopic visualization for stained CTCs. Single cells were individually micromanipulated using a 10 μm transfer tip on an Eppendorf TransferMan NK 2 micromanipulator, transferred into PCR tubes containing RNA protective lysis buffer, and flash frozen in liquid nitrogen. A total of 221 putative single CTCs were successfully isolated by micromanipulation (see Fig. S1C).

Single cell RNA sequencing

Complementary DNA (cDNA) was prepared from single cells, amplified and subjected to

library construction for transcriptome analysis using the ABI SOLiD platform, following published protocols (*31*), with slight modifications as previously described (*9*). Only cells passing quality control qPCR for GAPDH and beta-actin were subjected to library construction, followed by sequencing on the ABI 5500XL. RNA sequencing and digital gene expression profiling yielded an average of 4 to 5 million uniquely aligned reads per sample (Fig. S2A). Of the 133 single prostate CTCs that were successfully subjected to next generation RNA sequencing, 122 (92%) had greater than 100,000 aligned reads (Fig. S2A).

Bioinformatic analyses

RNA sequences from single cells, patient-derived leukocytes, and primary tumor samples were aligned to the known human transcriptome (hg19) using TopHat (*33*). Determination of Reads-Per-Million (RPM) and log10(RPM) were performed as previously described (*8*). The reads from dbGaP dataset phs000443.v1.p1 (*34*) were processed the same way with the exception that, since these samples were run on an Illumina GAII rather than a SOLiD sequencer, we first subjected the reads to the program trimmomatic's ILLUMINACLIP TruSeq2-SE.fa function to remove the adapter and other Illumina-specific sequences from the read. Unsupervised clustering analysis was performed using agglomerative hierarchical clustering with average linkage (Fig. 1A).

For independent validation of the quality of our single cell RNA-seq data, we confirmed the expression of a panel of genes in a subset of isolated single prostate CTCs using an independent methodology, single cell multiplex qRT-PCR (Fluidigm Biomark), as previously described (*10*) (Fig. S2D). In addition, we compared a list of genes that were highly upregulated in primary tumors in our RNA-seq data set with the expression profiles of these same genes in a previously published RNA-seq data set that included primary and metastatic prostate tumors (dbGaP dataset phs000443.v1.p1) (*34*) (Fig. S3). This analysis showed that genes that were highly expressed in primary tumors compared to CTCs in our data set were also highly expressed in primary tumors compared to metastases in the previously published data set.

Thresholding to select lineage-confirmed CTCs

Stringent expression thresholds were used to define lineage-confirmed CTCs, in order to exclude specimens containing contaminating leukocytes and ensure analysis of bonafide prostate CTCs (Fig. S2B). For each specimen we let its y-value be the maximum of its log10(RPM) for CD45 and CD16 (leukocyte markers) and let its x-value be the maximum of its log10(RPM) for KRT7, KRT8, KRT18, KRT19, EPCAM, AR, KLK3 (PSA), FOLH1 (PSMA) and AMACR (prostate-specific and epithelial markers). We defined an x-threshold as the midpoint between the maximum x-value of the white blood cells and the minimum x-value of the prostate cell lines. We defined a y-threshold as the midpoint between the minimum y-value of the white blood cells and the maximum y-value of the prostate cancer cell lines. We designated a candidate CTC as lineage-confirmed if its x-value was greater than the x-threshold and its y-value was less than the y-threshold.

Heterogeneity

To compare heterogeneity within and between subsets of specimens, we used means of correlation coefficients and jackknife estimates as follows. Determine the 2000 genes with the highest variance in log10(RPM) values across all specimens. Let v_i denote the log10(RPM) values for those 2000 genes for the i^{th} specimen and let $c(i, j)$ denote the Pearson correlation coefficient between v_i and v_j. Given T, a subset of the set of pairs of specimens, we let

$$M_T = \underset{(i,j)\in T}{\text{mean}}(\text{atanh}(c(i, j))).$$

Let s_T be the jackknife estimator of the standard deviation of M_T, where the jackknife is with respect to specimens (not pairs of specimens). We then call $\tanh(M_T)$ the "mean correlation coefficient" and define its 95% confidence interval to be $\tanh(M_T \pm s_T\Phi^{-1}(0.975))$, where Φ is the cumulative distribution function of the standard normal distribution. Given two subsets of the set of pairs of specimens, T and U, to compute a p-value for the null hypothesis that the mean of M_T is the same as the mean of M_U, we let

$$p = 2\left(1 - \Phi\left(\left|M_T - M_U\right| / \sqrt{s_T^2 + s_U^2}\right)\right).$$

To consider whether there's a significant difference between the heterogeneity in cell lines and CTCs, we let T be (i, j) such that $i > j$ and specimens i and j are cells from the same cell line and let U be (i, j) such that $i > j$ and specimens i and j are CTCs from the same patient. To consider whether there's a significant difference between the within-patient heterogeneity and the between-patient heterogeneity, we let T be (i, j) such that $i > j$ and specimens i and j are CTCs from the same patient and we let U be (i, j) such that $i > j$ and specimens i and j are CTCs from different patients.

Differential gene expression

Supervised differential gene expression was performed for the datasets shown in Fig. S5 and Table S4. For each RNA-seq dataset, we first filtered out genes for which the 0.9 quantile of RPM values was less than 10. For each microarray dataset, we first filtered out genes for which the 0.9 quantile of unlogged expression units per million was less than 10. A t-test assuming equal variance in the two classes was then performed for each gene on the log10(RPM) values for the RNA-seq datasets and on the GEO-provided expression values for the microarray datasets. The resulting p-values were used to create False Discover Rate (FDR) estimates by the Benjamini-Hochberg (BH) method. A gene was considered differentially expressed if its FDR estimate was less than 0.1 and its fold-change was greater than 2.

Gene set enrichment

Enrichment of signaling pathways in the differentially expressed genes was determined by performing a hypergeometric test for gene sets in the Pathway Interaction Database (PID) (*15*). When considering multiple gene sets, the resulting p-values were used to estimate FDR by BH. When determining pathways differentially expressed in CTCs versus primary tumors but not in metastatic tumors (Fig. 2C and 2D), to be conservative

in pathways we identified as uniquely enriched in CTCs, we used an FDR threshold of 0.1 for the CTC versus primary tumors comparison and 0.25 for the metastatic versus primary tumors comparisons.

GSEA version gsea2-2.0.14 was run first on the PID gene sets from version 4.0 of MSigDB (*35*) to generate hypotheses (Fig. 3B, upper panel) and later on specific gene sets to test hypotheses (Fig. 3B, lower panels and Fig. 4D). For right panels of Fig. 4D, we considered samples in GEO GSE52169 to be resistant and GR-high if their title began with "Res - top 50th percentile of GR expressers" or "Res - top 75th percentile of GR expressers." Those whose title began with "Res - Low GR" we considered to be resistant and GR-low.

Androgen receptor (AR) splice variants

To look for evidence of the AR splice variants discussed in Egan et al. (*1*), we consulted Lu and Luo (*17*) for genomic locations of the cryptic exons. We then added the splice variants found in Figure 3 of Egan et al. (*1*) to the transcriptome we had used for aligning and re-aligned. We then submitted the resulting new alignments to cufflinks (*33*) to quantify the different AR splice variants. We found that the 3'-biased nature of our reads caused cufflinks to output very wrong interpretations since cufflinks interprets a lack of reads in a location as evidence against any splice variant that should have reads at that location. So, we decided to only look for positive evidence of AR splice variants. We counted reads spanning exons 4 and 8 or spanning exons 8 and 9 (see Figure 1 of Lu and Luo (*17*) as evidence of AR^{v567es} (AR-V12). We normalized these counts by the total number of reads that spanned exons in that specimen. We counted reads aligning to cryptic exon CE3 to be evidence of AR-V7 and reads aligning to cryptic exons CE4 or CE1 to be evidence of AR-V1, AR-V3 or AR-V4. These counts of alignments to cryptic exons were normalized by the total number of aligned reads for that specimen.

KLK3 splice variants

To look for evidence of KLK3 splice variants we added the splice variants found in Figure 6 of Kurlender et al. (*23*) to the transcriptome we had used for aligning and then re-aligned. We counted reads overlapping the introns in that figure as evidence of the splice variants that contain sequence from those introns as indicated in the figure (after noting that the second variant labeled NA in the figure has since been named NM_001030047 and the third variant labeled NA in the figure has since been named NM_001030048). These counts of alignments to introns were normalized by the total number of uniquely aligned reads for that specimen.

AR mutations

To look in our single-cell RNA sequencing data for evidence of known prostate-related mutations in the AR, we downloaded the Androgen Receptor Gene Mutations Database (*16*) as available at http://androgendb.mcgill.ca on June 12, 2014. We filtered the database as follows. We kept only those entries with the word "Prostate" in the "Phenotype" column. We knew that our alignment had yielded no insertions or deletions in the AR, so we kept only those entries for which the "Mutation type" column was "Substitut.". We then kept only those entries for which the "To nucleotide" column was

">A", ">C", ">G", or ">T" and for which the "nucleotide position" field was present. We also fixed the record with accession number 568 to have "nucleotide position" equal to 2688 and "From nucleotide" set to "2688G". We then removed records that had the same "nucleotide position" as previous records. Finally, we added the F876L mutation (*19, 20*) (which in NM_000044.2 (the version of AR used in the database) is at amino acid 877 and is a T -> C substitution at nucleotide 3744).

For each mutation in the database and each single-cell specimen, we counted how many reads aligned to the position, how many were wild-type, and how many were the "To nucleotide" from the database. In order to determine which mutations were statistically significant, we needed an estimate of the error rate of our sequencing procedure. Since the AR is on the X chromosome and we are only considering single cells, we expected the reads at a particular location to be almost all wild-type or almost all not wild-type. Indeed, we found this to be the case. Only two location/specimen pairs had a percentage of wild-type reads between 10% and 85%. The 3068 other location/specimen pairs had a percentage of wild-type reads less than 10% or greater then 85%. We assumed, therefore, that the location/specimen pairs with percentage of wild-type reads greater than 85% were, in fact, wild-type and that any non-wild-type read was an error. This gave us an error rate estimate of 0.0012. For each location/specimen pair, we then did a one-sided binomial test with alternative hypothesis being that the probability of getting the substitution listed in the database is greater than 0.0012. We adjusted all the resulting p-values for multiple hypothesis testing using the Holms method. We concluded there was a mutation at those location/specimen pairs for which the adjusted p-value was less than 0.05 and the percentage of reads that matched the mutation in the database was greater than 90%.

Metagene computation

If we let $x_1, x_2, \ldots, x_m$ be the log10(RPM) values of the UP genes of a signature and let $y_1, y_2, \ldots, y_n$ be the log10(RPM) values of the DOWN genes of that signature, we define the metagene to be $(x_1 + x_2 + \ldots + x_m - y_1 - y_2 - \ldots - y_n)/(m+n)$. The UP and DOWN genes of the signatures for which we computed metagenes are given in Table S7.

P-values for Group A vs. Group B

The "CTC" p-values were computed by a two-sided t-test with Welch approximation to the degrees of freedom applied to the log10(RPM) values of Group A specimens versus those of Group B specimens. The "patient" p-values were determined by fitting the mixed effects model

$$e_{i,j} = \beta_0 + \beta_1 I_i + b_i + \varepsilon_{i,j},$$

where $e_{i,j}$ is the log10(RPM) value of the jth specimen from the ith patient, I_i is 0 if the ith patient is in Group A and 1 otherwise, $b_i \sim N(0, \sigma_b^2)$ and $\varepsilon_{i,j} \sim N(0, \sigma^2)$. The "patient" p-value was defined as the two-sided p-value for the null hypothesis $\beta_1 = 0$ as determined by the lme function of the R package nlme.

P-values for KLK3 splice variants in primary tumors vs. CTCs
For each sample, we summed the counts described in the "KLK3 splice variants" paragraph above and then normalized the sum by the total number of uniquely aligned reads. "CTC" p-values and "patient" p-values were then computed as in the "P-values for Group A vs. Group B" paragraph above.

RNA In-Situ Hybridization (RNA-ISH)

RNA-ISH in prostate tumor tissues
RNA in situ Hybridization (RNA-ISH) was performed using the Affymetrix ViewRNA ISH Tissue Assay Kit (2-plex). Briefly, paraffin-embedded tissue blocks were freshly cut and frozen at -80°C until staining. Upon removal from the freezer, slides were baked for 1 hr at 60°C. Slides were treated with Histo-Clear to remove paraffin. Tissue sections were pretreated in pretreatment buffer solution for 10 min at 95°C and digested with protease for 10 min, before being fixed at RT in 5% formaldehyde. Target probe sets were applied and hybridized to the tissue by incubating for 2 hr at 40°C. Type 1 WNT5A (VA1-12202) was used at 1:50, and Type 6 probes KRT8, KRT18, and KLK3 (when used) (VA6-11560, VA6-11561, VA6-13505) pooled each at 1:200. Signal was amplified through the sequential hybridization of PreAmplifier and Amplifer QT mixes to the target probe set. Target mRNA molecules were detected by applying Type 6 Label Probe with Fast Blue substrate and Type 1 Label Probe with Fast Red substrate. Tissue was counterstained with Gill's Hematoxylin for 10 sec at RT. DAPI (Invitrogen, D3571; 3.0 μg/ml) staining was performed for 1 min. Slides were imaged on the Aperio microscopy system within 1 week of staining to maintain a digital pathology archive of specimens.

RNA-ISH in circulating tumor cells
Isolated CTCs were centrifuged onto poly-L-lysine coated glass slides (Sigma Life Sciences, P0425) for 5 minutes at 800 rpm using Shandon EZ Megafunnels (A78710001). Slides were dried for 10 minutes, fixed with 4% PFA for 10 minutes and washed with 1xPBS for 10 minutes before dehydration and storage in 100% ethanol at -20 degrees Celsius until staining procedure. ViewRNA ISH Cell Assay Kit (Affymetrix, Santa Clara, CA) was used to stain CTC slides. Cells were permeabilized using Detergent Solution QC for 5 minutes at room temperature (RT). RNA was unmasked using Protease QS (1:2000 dilution) for 10 minutes at RT. Type 1 probes for WNT5A (VA1-12202), WNT7B (VA1-16571) and Type 6 probes for KRT8 (VA6-11560), KRT18 (VA6-11561), KRT19 (VA6-10947), KLK3 (VA6-63528), FOLH1 (VA6-11578), EPCAM (VA6-13003) were hybridized to target mRNA for 3 hours at 40°C. Signal amplification was achieved through sequential hybridization of Pre-Amplifier molecules, Amplifier molecules, and fluorescently conjugated Label Probe oligonucleotides. Cells were stained with DAPI (Invitrogen, D3571; 5 μg/ml) for 1 min at RT. Slides were then scanned on the BioView automated fluorescent imaging platform for quantification and analysis.

Cell line experiments

Prostate cancer cell lines (LNCaP, VCaP, PC3, DU145) were obtained from ATCC after authentication by short tandem repeat profiling, and maintained as recommended. Drug treatment experiments were performed using 1-10 μM enzalutamide (Selleckchem), 1 nM R1881 (Perkin-Elmer), or dimethyl sulfoxide (DMSO). Sequenced LNCaP cells labeled LNCaP.R or LNCaP.D were cultured for 3 days in medium containing 10% charcoal-stripped FBS (Invitrogen), and treated with R1881 or DMSO as a vehicle control for 24 hours. The enzalutamide-resistant cell line LN_EnzR was generated by prolonged (4 months) *in vitro* selection in the presence of 1 μM enzalutamide. Non-canonical Wnt ligands (*WNT4*, *WNT5A*, *WNT7B*, and *WNT11*) were overexpressed in LNCaP cells using lentiviral constructs. WNT4, WNT5a, WNT7b, WNT11 plasmids were purchased from Addgene (*36, 37*) (35873, 35874, 35878, 35885), and cloned into pLX301 (Addgene 25895) through Gateway Cloning (Life Technologies). pLX301-Wnt plasmids together with packaging plasmids were transfected into 293T cells using Lipofectamine 2000 (Life Technologies). Lentivirus was collected 48 and 72 hours later. LNCaP cells were infected with lentivirus in the presence of 8mg/ml polybrene overnight. Stable cell pools were selected in growth medium containing 2 mg/mL puromycin for 1 week.

siRNA
Knockdown experiments of endogenous *WNT5A* and *WNT7B* gene expression in cells were performed using siRNA. ON-TARGETplus siRNAs against *WNT5A*, *WNT7B*, and control siRNAs were purchased from GE Dharmacon.

Western blots
Wnt5a (C27E8) antibodies were purchased from Cell Signaling. Antibodies against Wnt7b (ab155313) and Wnt11 (ab96730) were purchased from Abcam. Antibodies against GAPDH (MAB374) were acquired from Millipore. Goat anti-rabbit or anti-mouse antibodies conjugated to IRDye 800CW were used as secondary antibodies (Cell Signaling) and detected by Li-cor Odyssey CLX Infrared Imaging System.

Primers and quantitative real-time PCR
Total RNA was extracted using RNeasy Micro Kit (Qiagen). 1μg of RNA was used to generate cDNA using superscript III First Strand synthesis system (Life Technologies). Reactions were amplified and analyzed in triplicate using the ABI 7500 Real-Time PCR System. The following primers are listed in the below table:

WNT4_F	TCTGACAACATCGCCTACG
WNT4_R	CGTCTTTACCTCACAGGAGC
WNT5A_F	ATTCTTGGTGGTCGCTAGGTA
WNT5A_R	CGCCTTCTCCGATGTACTGC
WNT7B_F	TTTCTCTGCTTTGGCGTCC
WNT7B_R	TACTGGCACTCGTTGATGC
WNT11_F	AGCCAATAAACTGATGCGTC
WNT11_R	ACAGGTATCGGGTCTTGAG
GAPDH_F	GGTCTCCTCTGACTTCAACA
GAPDH_R	GTGAGGGTCTCTCTCTTCCT

Cell growth and colony formation assay

For proliferation assays, subconfluent cells were plated in triplicate for each time point at a density of 2,000 cells per well of 96-well plates 24 hours after siRNA transfection. The fold increase in cell number was measured by the CellTiter-Glo Luminescent Cell Viability Assay (Promega). For colony formation assays, cells were plated in triplicate at a density of 10,000 cells per well of 12-well plates in the presence of 1μM, 3μM or 10μM Enzalutamide (Selleckchem), and grown for 21 days before fixing and staining with crystal violet (Sigma-Aldrich). Fresh medium containing enzalutamide was changed twice a week.

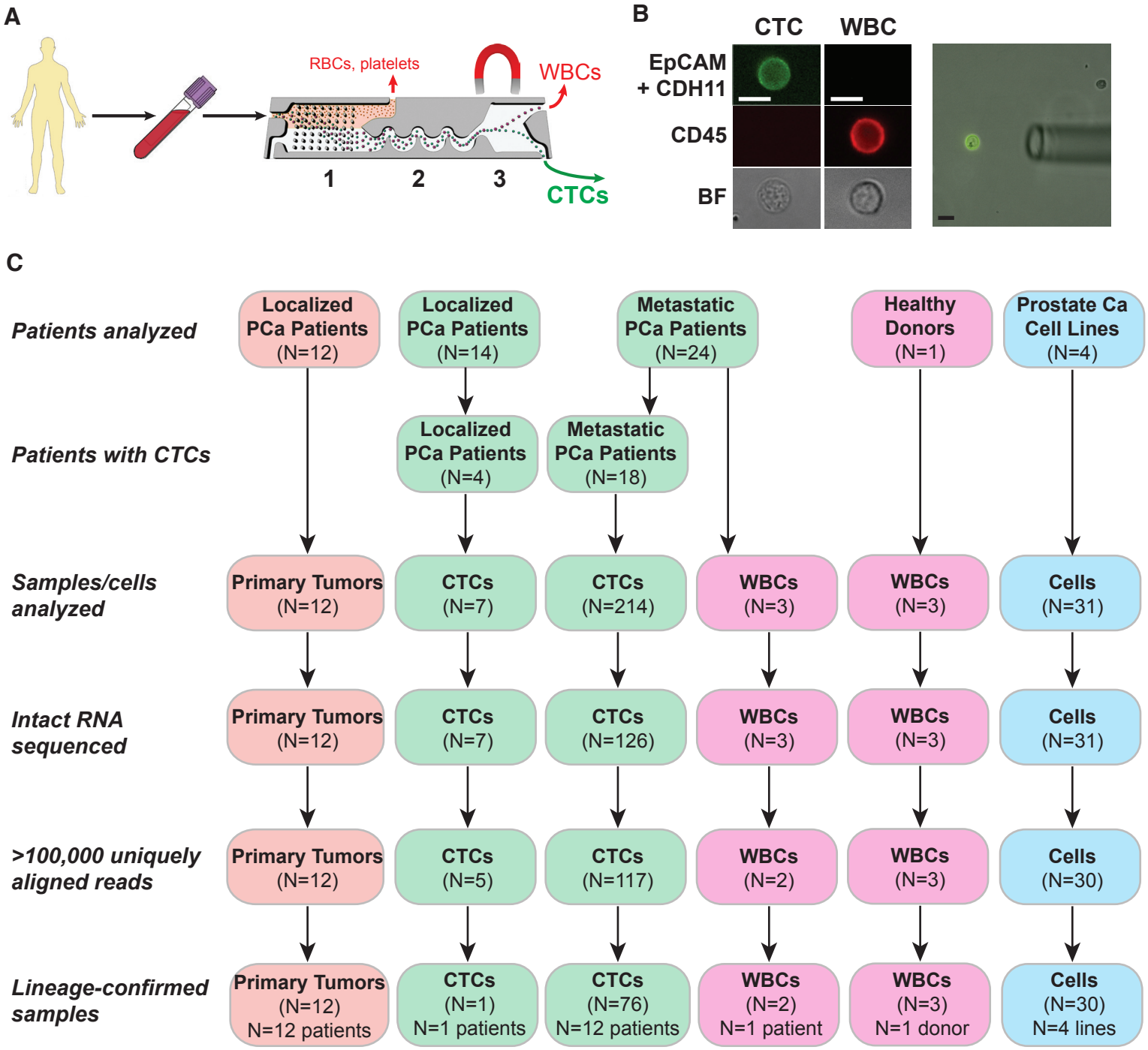

Fig. S1. Experimental workflow for single CTC RNA-sequencing studies. **(A)** Schematic of integrated microfluidic system (CTC-iChip) to deplete hematopoietic cells from whole blood and isolate circulating tumor cells (CTCs). The three microfluidic components of the system are depicted, including (i) hydrodynamic sorting to enrich for nucleated cells (CTCs and WBCs), (ii) inertial focusing to align all nucleated cells within a single streamline for efficient sorting, and (iii) magnetophoresis to remove leukocytes tagged with immunomagnetic beads. **(B)** Immunofluorescence images of a CTC stained with antibodies against both EpCAM and CDH11 (green), and a leukocyte (WBC) stained with antibody against CD45 (red). Bright field (BF) image of the CTC and WBC. Right panel depicts a CTC being isolated using a micromanipulator needle. Scale bars = 10 μm. **(C)** Flow chart of samples analyzed in this study. For CTC samples, patients were analyzed for the presence of CTCs by immunofluorescence microscopy as above, and single CTCs were micromanipulated and processed for RNA sequencing. Lineage-confirmed CTCs were defined as those that met stringent pre-specified thresholds for expression of prostate cancer-specific markers and low expression of leukocyte markers (see Fig. S2B, Results, and Methods).

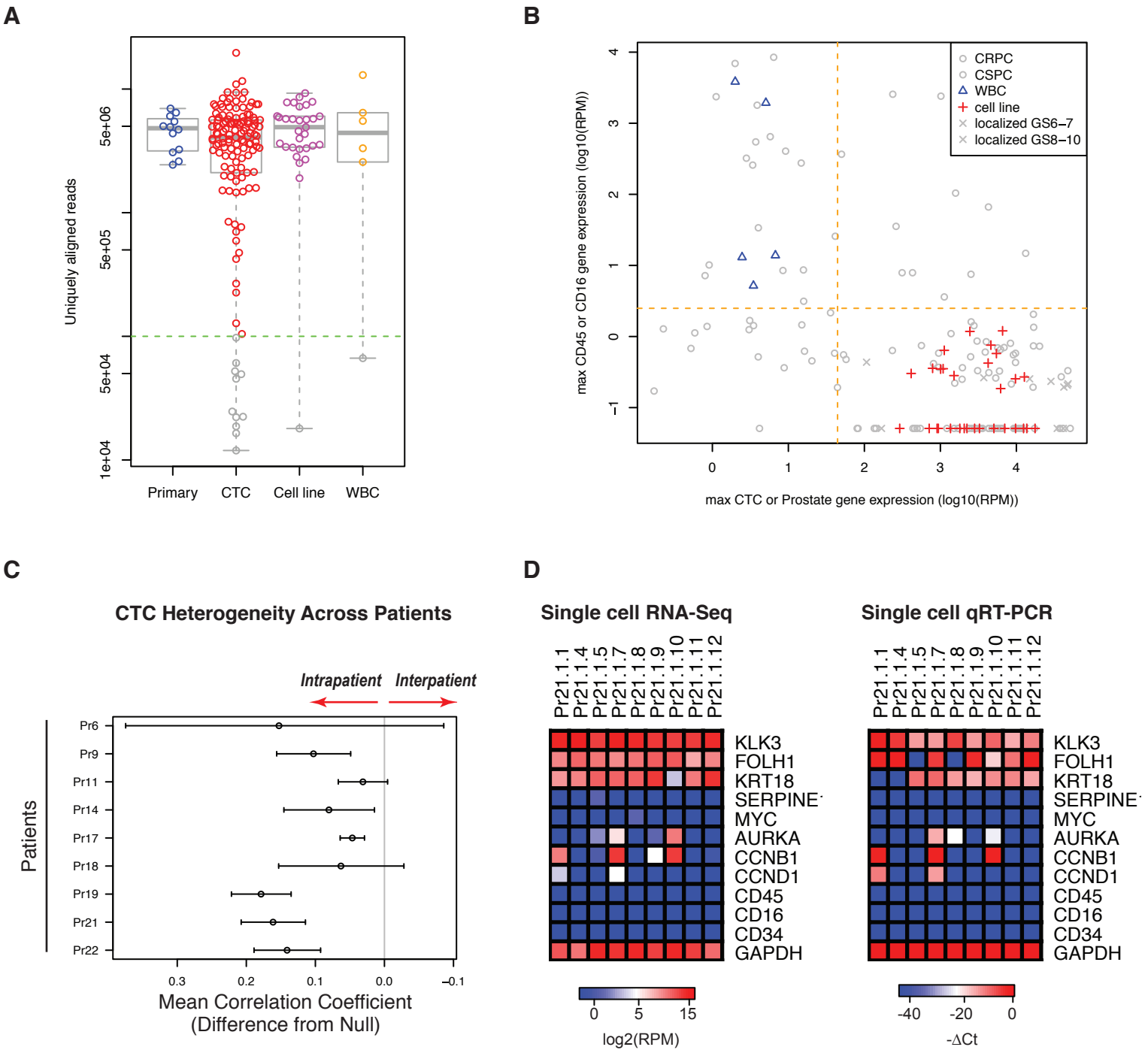

Fig. S2. RNA-sequencing of single CTCs, primary prostate tumors, cell lines, and leukocytes. **(A)** Uniquely aligned RNA-sequencing reads for primary prostate tumors, single candidate CTCs, prostate cancer cell lines, and leukocytes. Dotted line represents the cutoff value of 100,000 uniquely aligned reads, and samples below this threshold were not further analyzed. **(B)** Stringent expression thresholds used to define lineage-confirmed CTCs. Maximum log10(RPM) expression of CTC or prostate specific markers (KRT7, KRT8, KRT18, KRT19, EPCAM, AR, KLK3, FOLH1, and AMACR) are plotted against leukocyte markers (CD45 and CD16). Dashed lines are thresholds defined by the relative expression of these markers in leukocytes and prostate cancer cell lines. CTCs in the lower right quadrant were defined as lineage-confirmed CTCs. See Methods for details. **(C)** CTC heterogeneity across patients, illustrated by the difference between the mean correlation coefficients within patients (intrapatient) and between patients (interpatient) (see Fig. 1, B and C). **(D)** Validation of single cell RNA-seq data using an independent method (single cell multiplex qRT-PCR) in a subset of isolated single prostate CTCs with a panel of selected genes (prostate-specific genes, leukocyte genes, and cell cycle genes).

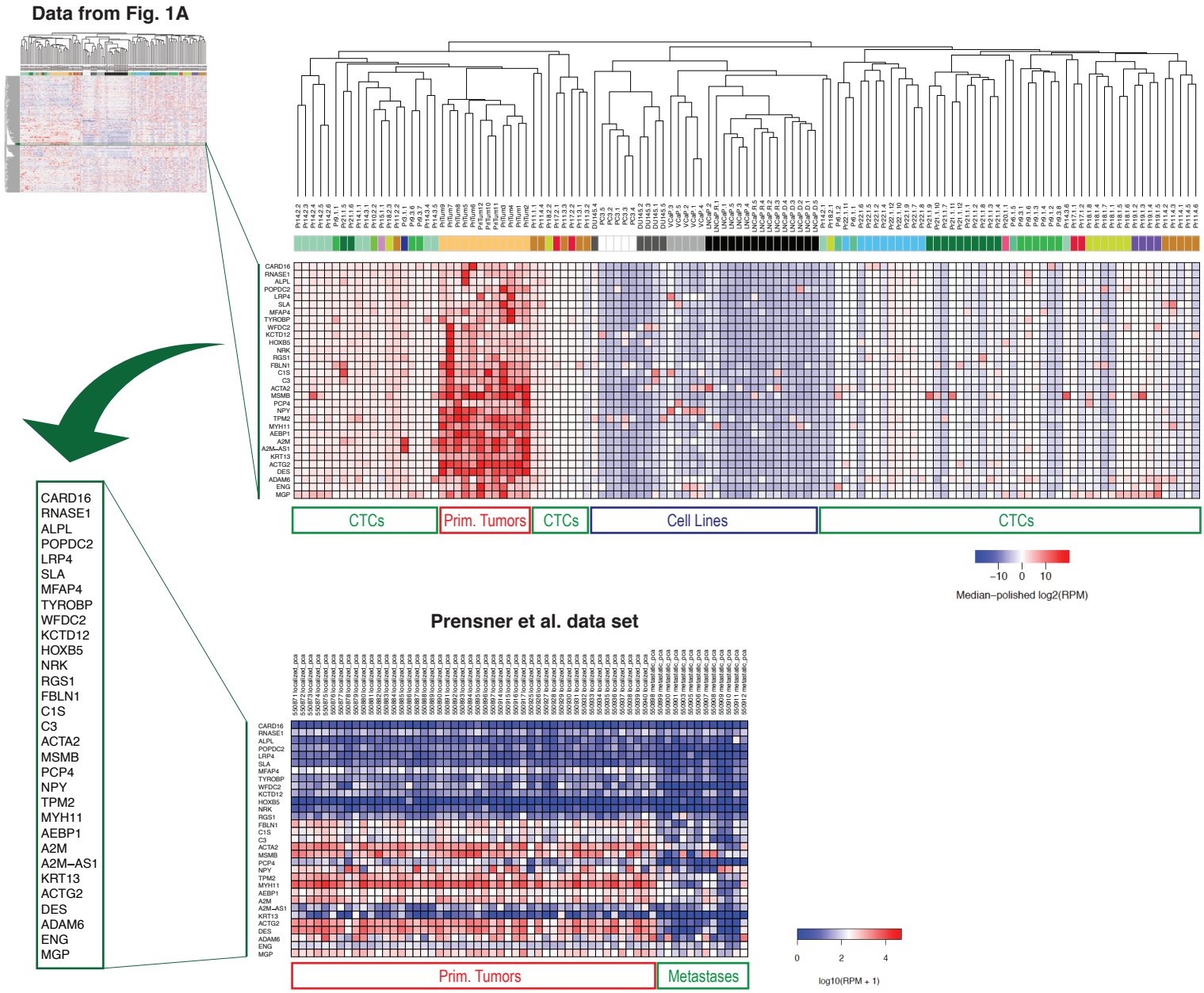

Fig. S3. Confirmation of selected gene expression profiles using an independent RNA-seq data set. Top panel, magnified view of the heatmap from Fig. 1A, revealing a set of genes that are highly upregulated in primary tumors. Bottom panel, expression profiles of these same genes in a previously published RNA-seq data set (dbGaP dataset phs000443.v1.p1) that included primary and metastatic prostate tumors (34).

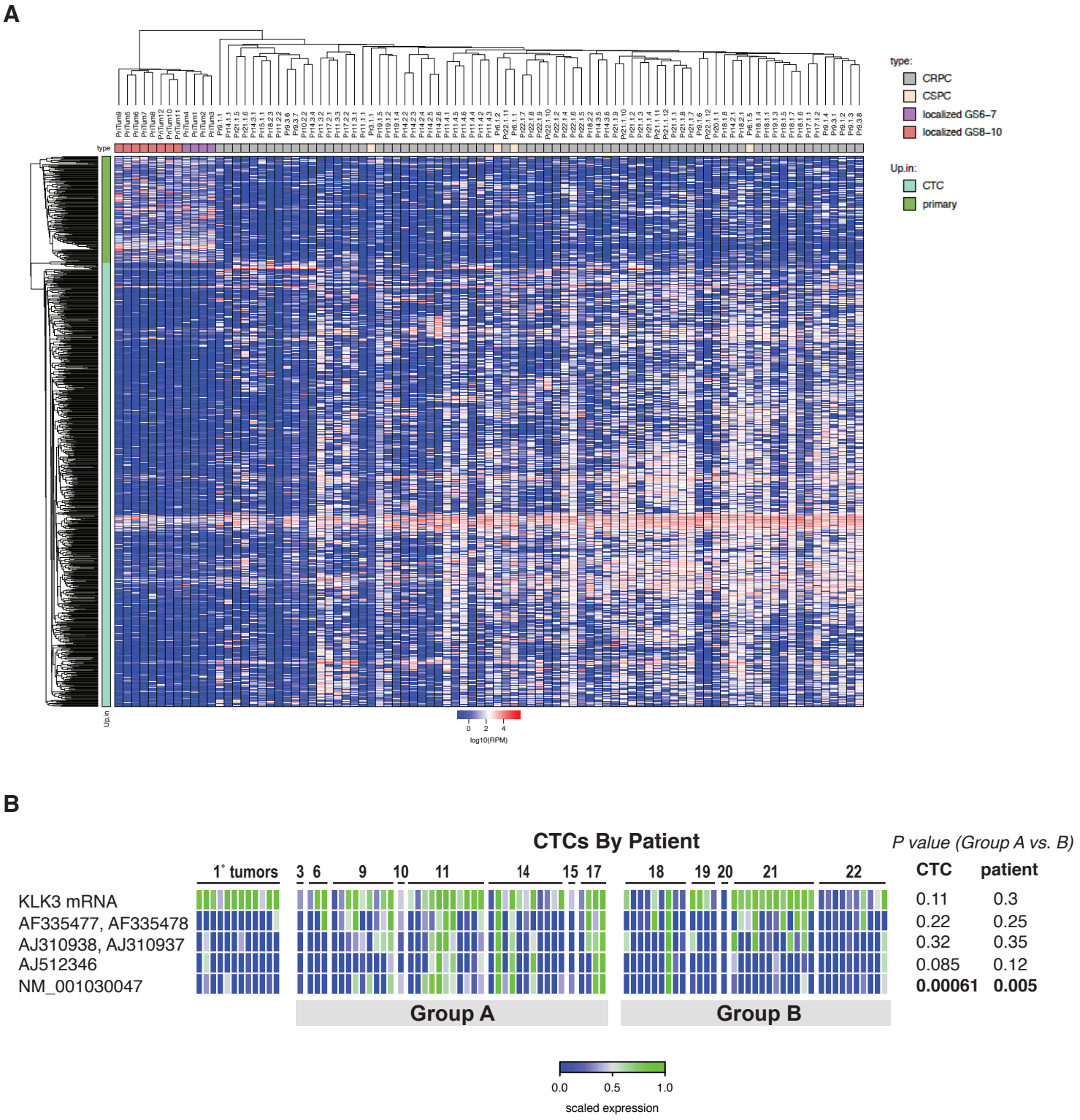

Fig. S4. (A) Comparison of prostate CTCs and primary prostate tumors by unsupervised hierarchical clustering. CRPC, castration-resistant prostate cancer; CSPC, castration-sensitive prostate cancer; GS, Gleason score. **(B)** Heat map depicting KLK3 splice variants in radical prostatectomy specimens, prostate CTCs from enzalutamide-naïve patients (Group A), and prostate CTCs from patients who had radiographic or biochemical progression of disease while receiving treatment with enzalutamide (Group B). Numbers at top of heatmap represent ID numbers (Pr numbers) for patients from which each CTC is derived.

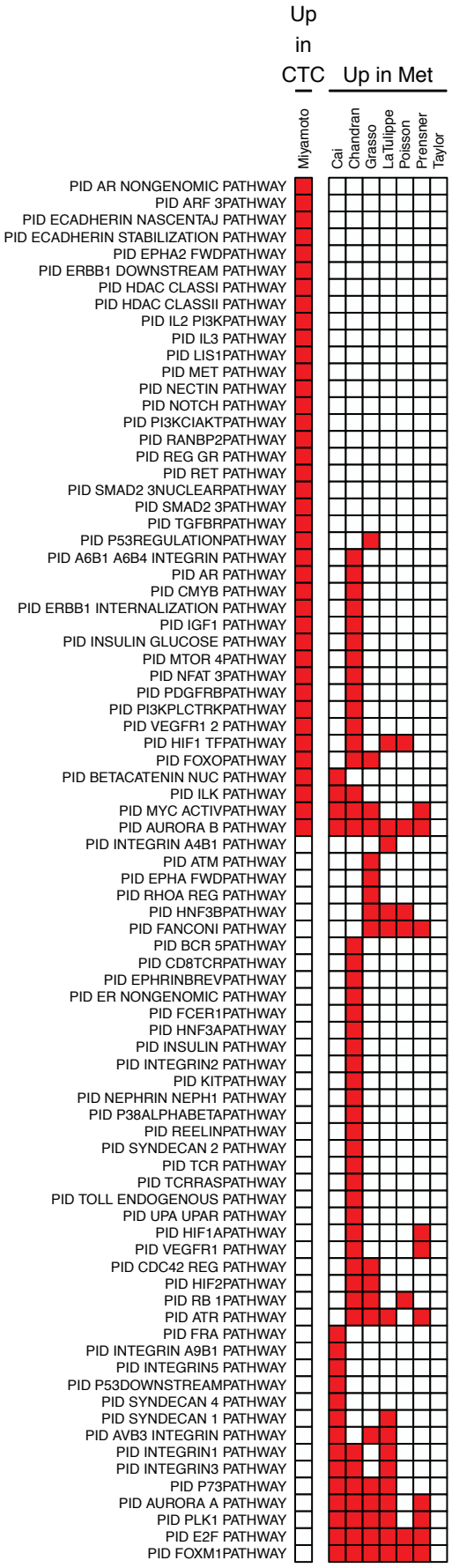

Fig. S5. Heatmap showing PID pathways enriched in prostate CTCs compared to primary tumors in the current study (Miyamoto), and PID pathways enriched in metastatic tumors compared to primary tumors in seven other datasets (see Table S4 and Methods).

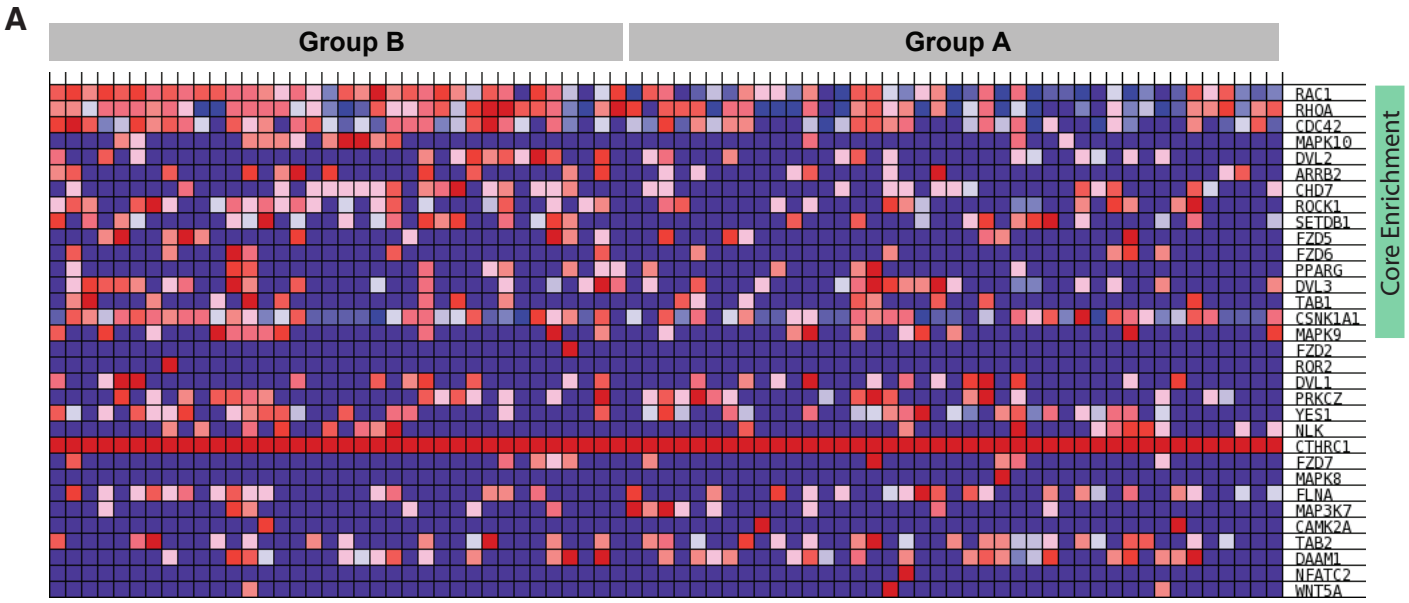

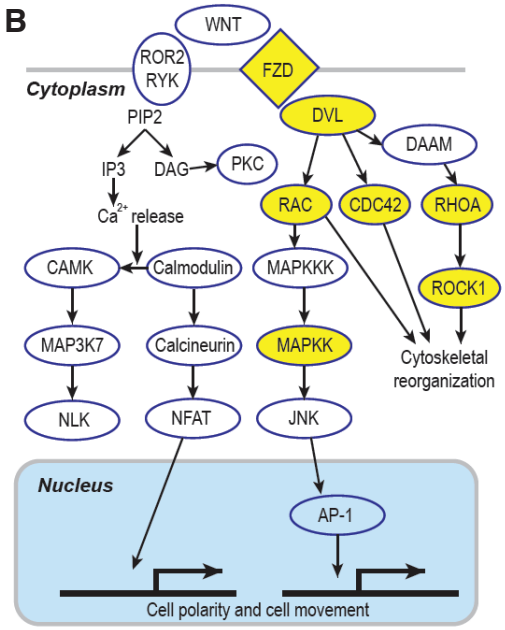

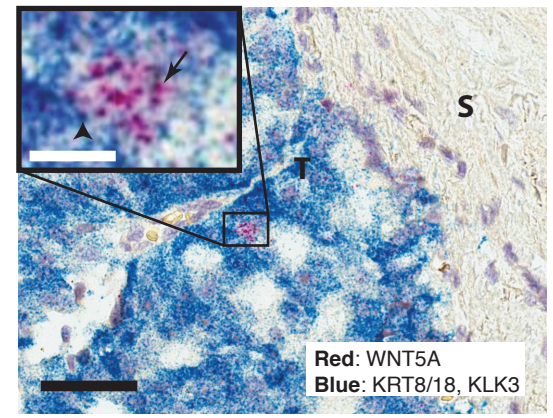

Prostate cancer	ncWNT expression (RNA-ISH)
Localized tumor (stromal cells) (N = 9 pts)	WNT5A: 0/416 cells (<0.2%) WNT7B: 2/459 cells (0.5%)

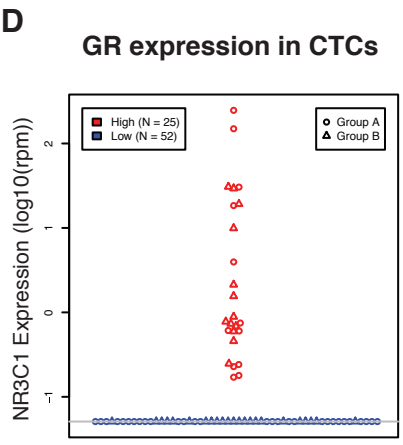

Fig. S6. Comparison of CTCs from Group A patients (enzalutamide-naïve) and Group B patients (progression while on enzalutamide). **(A)** Heat map corresponding to GSEA plot (Fig. 3B) showing enrichment of PID non-canonical Wnt pathway in CTCs from Group B compared to Group A patients, with Core Enrichment genes identified. **(B)** Non-canonical Wnt signaling pathway. Components of the pathway enriched in Group B compared to Group A based on GSEA analysis are highlighted in yellow. **(C)** Representative micrograph of RNA-in situ hybridization assay in primary prostate tumors, probing for WNT5A (red dots), and CK8, CK18, and KLK3 (blue dots). WNT7B probe was used in adjacent tissue sections (see Fig. 3C). T, tumor; S, stroma. 40x magnification, black scale bar = 50 µm. Inset, high magnification, white scale bar = 10 µm. **(D)** NR3C1 (GR gene) expression in single cell prostate CTC RNA-seq data.

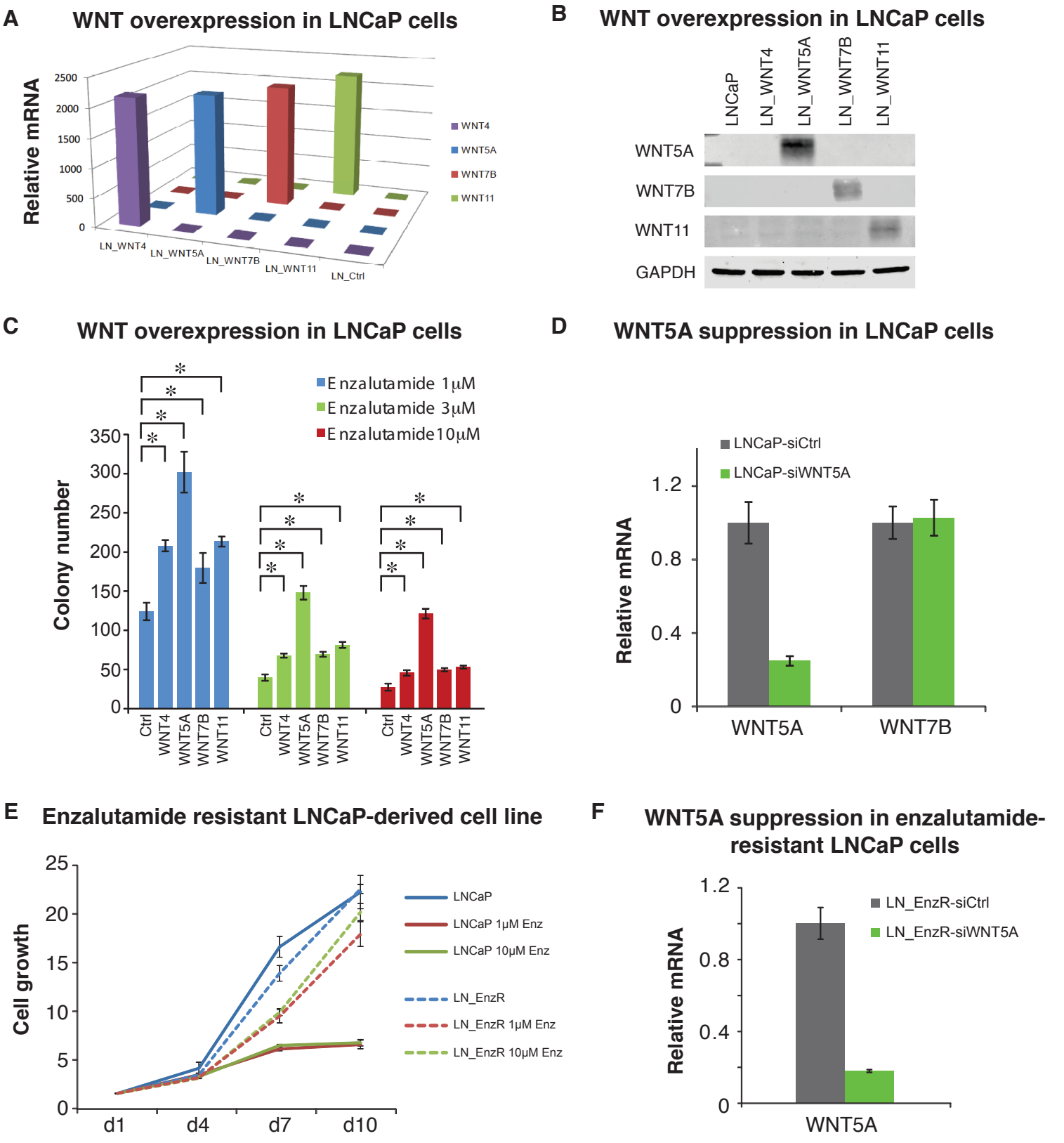

Fig. S7. Overexpression and knockdown of non-canonical (nc) Wnt in prostate cancer cell lines. **(A)** Stable ectopic expression of ncWnt ligands WNT4, WNT5A, WNT7B, WNT11 in LNCaP cells, quantified by qRT-PCR. **(B)** Western blot showing stable expression of WNT5A, WNT7B, WNT11 in LNCaP cells. No specific WNT4 antibody was available for the analysis. **(C)** Ectopic expression of ncWnts in LNCaP cells increases cell survival in the presence of different concentrations of enzalutamide. **(D)** Efficient knockdown of WNT5A in LNCaP cells using siRNA quantified by qRT-PCR. mRNA levels of WNT7B is not affected. **(E)** Growth curve demonstrating that the LNCaP-derived enzalutamide-resistant LN_EnzR cells shows continued growth in the presence of 1μM and 10μM enzalutamide, relative to control LNCaP cells. **(F)** Efficient knockdown of WNT5A in LN_EnzR cells quantified by qRT-PCR. Each experiment (C-F) was performed ≥3 times. Data are presented as mean +/- SD.

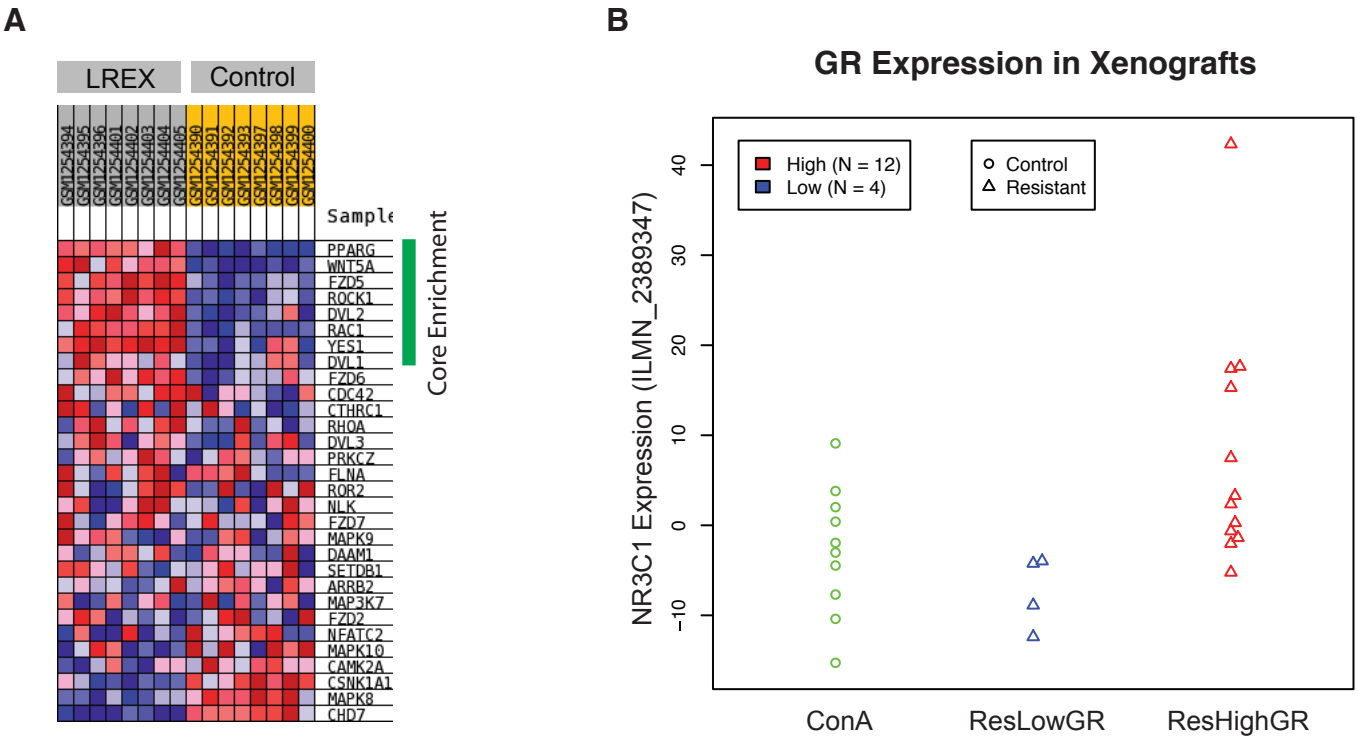

Fig. S8. GR expression in mouse xenografts. **(A)** Heat map corresponding to GSEA plot (Fig. 4D) showing ncWnt pathway enrichment in mouse xenografts derived from enzalutamide-resistant LREX' cells (29) compared to control LNCaP cells, with Core Enrichment genes identified. **(B)** NR3C1 (GR gene) expression in mouse xenograft microarray data from GEO GSE52169 (29).

Table S1 | Patient CTC Samples

Patient	Stage	Disease status at time of CTC collection	PSA (ng/mL)	No. cells picked	No. cells sequenced	No. lineage-confirmed CTCs	Group	Response to enzalutamide	Prior Treatments
Pr1	loc.	CSPC, pre-treatment	10.0	1	1	0	-	-	none
Pr2	loc.	CSPC, pre-treatment	6.8	2	2	0	-	-	none
Pr3	loc.	CSPC, pre-treatment	8.5	2	2	1	A	enzalutamide-naïve	none
Pr4	loc.	CSPC, pre-treatment	10.1	2	2	0	-	-	none
Pr5	met.	CSPC, pre-treatment	144.1	4	3	0	-	-	none
Pr6	met.	CSPC, pre-treatment	207.8	9	5	3	A	enzalutamide-naïve	none
Pr7	met.	CSPC, pre-treatment	34.7	3	2	0	-	-	none
Pr8	met.	CSPC, pre-treatment	7.3	5	5	0	-	-	none
Pr9	met.	CRPC, on abiraterone	93.9	32	17	9	A	enzalutamide-naïve	ADT
Pr10	met.	CRPC, on abiraterone	445.5	8	6	1	A	enzalutamide-naïve	ADT, doc, cabo
Pr11	met.	CRPC, on abiraterone	1504.0	27	15	11	A	enzalutamide-naïve	ADT, bic, metformin, keto, cabo, doc
Pr12	met.	CRPC, on abiraterone	0.2	3	2	0	-	-	ADT
Pr13	met.	CRPC, on abiraterone	0.2	2	2	0	-	-	ADT
Pr14	met.	CRPC, on abiraterone	365.6	20	13	11	A	enzalutamide-naïve	ADT
Pr15	met.	CRPC, on docetaxel	43.0	4	2	1	A	enzalutamide-naïve	ADT, abi
Pr16	met.	CRPC, on Phase I drug†	87.7	8	6	0	-	-	ADT, metformin, keto, doc, abi, cabaz
Pr17	met.	CRPC, on cabazitaxel	384.9	7	4	4	A	enzalutamide-naïve	ADT, doc, abi
Pr18	met.	CRPC, on enzalutamide	311.3	27	13	9	B	Rad. progression	ADT, sipT, metformin, cabo, doc
Pr19	met.	CRPC, on enzalutamide	349.4	9	5	4	B	Rad. and PSA progression	ADT, abi, doc
Pr20	met.	CRPC, on enzalutamide	94.0	4	2	1	B	Rad. and PSA progression	ADT, doc, abi
Pr21	met.	CRPC, on enzalutamide*	4573.0	18	12	12	B	PSA progression	ADT, doc, abi, cabaz
Pr22	met.	CRPC, on enzalutamide	219.1	24	12	10	B	Rad. and PSA progression	ADT, abi
			Total:	**221**	**133**	**77**			

Legend: ADT, androgen deprivation therapy; abi, abiraterone; bic, bicalutamide; cabaz, cabazitaxel; cabo, cabozantinib; CRPC, castration-resistant prostate cancer; CSPC, castration-sensitive prostate cancer; doc, docetaxel; ket, ketoconazole; loc., localized; met., metastatic; PSA, serum prostate-specific antigen at time of CTC collection; Rad., radiographic; sipT, sipuleucel-T; †E7050 and E7080; *started enzalutamide on the day of the CTC blood draw.

Table S2 | Primary Tumor Samples

Patient	Stage	Clinical status	PSA (ng/mL)	Gleason score	T Stage
PriTum1	localized	CSPC	4.6	3+3=6	pT2c
PriTum2	localized	CSPC	5	3+3=6	pT2c
PriTum3	localized	CSPC	10.8	5+4=9	pT3ab
PriTum4	localized	CSPC	7	3+4=7	pT2c
PriTum5	localized	CSPC	13	5+4=9	pT3a
PriTum6	localized	CSPC	12.9	5+4=9	pT3a
PriTum7	localized	CSPC	6.7	5+4=9	pT3ab
PriTum8	localized	CSPC	10.7	4+4=8	pT3a
PriTum9	localized	CSPC	16.7	5+4=9	pT3a
PriTum10	localized	CSPC	8.6	4+5=9	pT3ab
PriTum11	localized	CSPC	4.96	4+5=9	pT3a
PriTum12	localized	CSPC	4.4	4+3=7	pT2c

Legend: PSA, serum prostate-specific antigen; CSPC, castration-sensitive prostate cancer

Supplementary Excel Tables

Table S3. Genes differentially expressed between CTCs and primary prostate tumors. "Up in CTC" tab – 711 genes enriched in CTCs. "Up in Primary" tab – 173 genes enriched in primary tumors.

Table S4. Data sets used in the differential gene expression and pathway analyses comparing metastatic and primary prostate tumors (see Figs. 2C and S5).

Table S5. Androgen receptor mutation analysis in prostate CTCs, primary tumors, and prostate cancer cell lines.

Table S6. Androgen receptor splice variant analysis in prostate CTCs and primary tumors.

Table S7. Pathway signatures used for metagene analyses in this study (see Fig. 3A).

Supplementary References

32. H. Hieronymus, J. Lamb, K. N. Ross, X. P. Peng, C. Clement, A. Rodina, M. Nieto, J. Du, K. Stegmaier, S. M. Raj, K. N. Maloney, J. Clardy, W. C. Hahn, G. Chiosis, T. R. Golub, Gene expression signature-based chemical genomic prediction identifies a novel class of HSP90 pathway modulators. *Cancer Cell* **10**, 321–330 (2006).

33. C. Trapnell, A. Roberts, L. Goff, G. Pertea, D. Kim, D. R. Kelley, H. Pimentel, S. L. Salzberg, J. L. Rinn, L. Pachter, Differential gene and transcript expression analysis of RNA-seq experiments with TopHat and Cufflinks. *Nat. Protoc.* **7**, 562–578 (2012).

34. J. R. Prensner, M. K. Iyer, O. A. Balbin, S. M. Dhanasekaran, Q. Cao, J. C. Brenner, B. Laxman, I. A. Asangani, C. S. Grasso, H. D. Kominsky, X. Cao, X. Jing, X. Wang, J. Siddiqui, J. T. Wei, D. Robinson, H. K. Iyer, N. Palanisamy, C. A. Maher, A. M. Chinnaiyan, Transcriptome sequencing across a prostate cancer cohort identifies *PCAT-1*, an unannotated lincRNA implicated in disease progression. *Nat. Biotechnol.* **29**, 742–749 (2011).

35. A. Subramanian, P. Tamayo, V. K. Mootha, S. Mukherjee, B. L. Ebert, M. A. Gillette, A. Paulovich, S. L. Pomeroy, T. R. Golub, E. S. Lander, J. P. Mesirov, Gene set enrichment analysis: A knowledge-based approach for interpreting genome-wide expression profiles. *Proc. Natl. Acad. Sci. U.S.A.* **102**, 15545–15550 (2005).

36. R. Najdi, K. Proffitt, S. Sprowl, S. Kaur, J. Yu, T. M. Covey, D. M. Virshup, M. L. Waterman, A uniform human Wnt expression library reveals a shared secretory pathway and unique signaling activities. *Differentiation* **84**, 203–213 (2012).

37. X. Yang, J. S. Boehm, X. Yang, K. Salehi-Ashtiani, T. Hao, Y. Shen, R. Lubonja, S. R. Thomas, O. Alkan, T. Bhimdi, T. M. Green, C. M. Johannessen, S. J. Silver, C. Nguyen, R. R. Murray, H. Hieronymus, D. Balcha, C. Fan, C. Lin, L. Ghamsari, M. Vidal, W. C. Hahn, D. E. Hill, D. E. Root, A public genome-scale lentiviral expression library of human ORFs. *Nat. Methods* **8**, 659–661 (2011).